Phys. Lett. B 878 (2026) 140497

Contents lists available at ScienceDirect

Physics Letters B

journal homepage: www.elsevier.com/locate/physletb

Letter

Search for long-lived particles using displaced vertices of oppositely charged leptons in 140 fb^{-1} of pp collisions at $\sqrt{s} = 13$ TeV with the ATLAS detector

The ATLAS Collaboration [1]

ARTICLE INFO

Editor: Dr. M. Doser

ABSTRACT

A search is presented for long-lived particles decaying into an oppositely charged lepton pair, $\mu^+\mu^-$, e^+e^-, or $e^\pm\mu^\mp$, that form a vertex within the inner tracking system of the ATLAS detector at the Large Hadron Collider, displaced from the primary proton–proton interaction region. The analysis uses the 140 fb^{-1} of Run-2 data collected at $\sqrt{s} = 13$ TeV by the ATLAS experiment in 2015–2018. The results of the analysis are interpreted in the context of three benchmark models covering masses from 0.1 to 2.2 TeV and a range of mean proper lifetimes times the speed of light from 1 to 10 000 mm. The first model is a generic Z' boson pair-produced by a new heavy scalar, with the Z' decaying into lepton pairs. The remaining two models are R-parity violating supersymmetric models in which the lightest neutralino $\tilde{\chi}_1^0$ decays into $\ell^+\ell'^-\nu$ ($\ell, \ell' = e, \mu$). The models differ by the mode of production of the $\tilde{\chi}_1^0$, which can be produced via the decay of pairs of gluinos or of pairs of charginos and neutralinos ($\tilde{\chi}_1^\pm\tilde{\chi}_1^0$, $\tilde{\chi}_1^\pm\tilde{\chi}_2^0$, or $\tilde{\chi}_2^0\tilde{\chi}_1^0$). Although each benchmark sample includes pair-produced LLPs, only a single vertex is required to be reconstructed. No dilepton displaced vertex candidate is observed and the results are presented as upper limits on the production cross-sections. This analysis sets leading limits on the production cross-sections for multiple models, including parameter space that has never been directly probed.

1. Introduction

Searches for long-lived particles (LLPs) remain a well-motivated endeavor in the collider physics community. LLPs are a natural occurrence in many extensions of the Standard Model (SM), including Hidden Valley [1] models and various supersymmetric (SUSY) models like split supersymmetry, R-parity violating (RPV) SUSY [2,3], and gauge-mediated SUSY breaking models [4–6]. Their ubiquity is in part a result of the multiple possible means by which long lifetimes may arise, such as small couplings, small mass-splittings, and approximate symmetries. A neutral LLP can be detected indirectly by reconstructing its decay products, which may form a common vertex that is macroscopically displaced from the primary collision vertex.

This Letter presents the search for a heavy, long-lived, neutral particle whose decays include a dilepton pair ($\mu^+\mu^-$, e^+e^-, or $e^\pm\mu^\mp$) producing a displaced vertex (DV) that is reconstructed within the inner tracking system of the ATLAS detector [7] at the Large Hadron Collider (LHC) [8]. In this Letter, "leptons" refers to electrons and muons only. LLP decays into taus are not modeled or targeted by this analysis. The analysis uses 140 fb^{-1} of Run-2 data collected in proton–proton (pp) collisions at $\sqrt{s} = 13$ TeV between 2015 and 2018. Requirements are placed on reconstructed vertices to strongly suppress SM background, allowing for sensitivity to signal processes with small cross-sections.

Three benchmark models are considered. The first model simulates the production of a neutral, heavy scalar particle S that decays into a pair of long-lived Z' bosons that in turn decay into charged leptons. The second and third models are each simplified models motivated by the Minimal Supersymmetric Standard Model (MSSM) featuring a long-lived lightest neutralino that acquires its long lifetime due to a small RPV coupling and decays into two charged leptons and a neutrino. One of these MSSM-inspired RPV models features direct electroweakino production ($\tilde{\chi}_1^\pm\tilde{\chi}_1^0$, $\tilde{\chi}_1^\pm\tilde{\chi}_2^0$, or $\tilde{\chi}_2^0\tilde{\chi}_1^0$) and the other features pair-production of gluinos ($\tilde{g}\tilde{g}$), which each decay into two quarks and the long-lived neutralino.

Requirements on collision events are not tailored to these specific models and no requirements are imposed on missing transverse momentum or jets. To maintain as much model independence as possible the reconstructed vertices are permitted to have extra tracks in addition to the two signal lepton tracks.

A previous search by the ATLAS Collaboration for the same signature was performed on 32.8 fb^{-1} of data collected in 2015 and 2016, using a squark production model rather than the gluino or electroweakino

Contact: atlas.publications@cern.ch.
[1] Authors are listed at the end of this paper.

https://doi.org/10.1016/j.physletb.2026.140497
Received 12 January 2026; Received in revised form 14 April 2026; Accepted 28 April 2026
Available online 5 May 2026

production models used here [9]. The ATLAS Collaboration also searched for dimuon vertices reconstructed using only muon-spectrometer tracks, allowing longer proper lifetimes to be targeted, based on the same subset of Run-2 data [10]. Additionally, the ATLAS Collaboration searched for delayed dielectron and diphoton vertices reconstructed using only calorimeter information, targeting masses consistent with the Z or Higgs bosons [11]. The CMS Collaboration searched for displaced dilepton vertices in the inner tracking volume at $\sqrt{s} = 8$ TeV [12]. Using data collected at $\sqrt{s} = 13$ TeV, the CMS Collaboration searched for pairs of collimated, displaced muons reconstructed using only information from the muon system in events with missing transverse momentum [13] and for lower mass LLPs decaying into muon pairs using dedicated trigger streams [14]. Also using data collected at $\sqrt{s} = 13$ TeV, the LHCb Collaboration searched for lower mass dimuon vertices in 5.1 fb^{-1} of data [15]. Finally, the CMS Collaboration released results for a Run-3 search targeting displaced dimuon vertices using 36.6 fb^{-1} of $\sqrt{s} = 13.6$ TeV data [16]. This is the first published analysis from the ATLAS Collaboration to use the full Run-2 data at $\sqrt{s} = 13$ TeV for a search for dilepton displaced vertices and is the only search using full Run-2 data to include dimuon, dielectron, and electron-muon displaced vertices.

2. ATLAS detector

The ATLAS detector at the LHC covers nearly the entire solid angle around the collision point.[1] It consists of an inner tracking detector surrounded by a thin superconducting solenoid, electromagnetic and hadronic calorimeters, and a muon spectrometer incorporating three large superconducting air-core toroidal magnets.

The inner-detector system (ID) is immersed in a 2 T axial magnetic field and provides charged-particle tracking in the range $|\eta| < 2.5$. The high-granularity silicon pixel detector covers the vertex region and typically provides four measurements per track, the first hit generally being in the insertable B-layer (IBL) installed before Run 2 [17,18]. It is followed by the SemiConductor Tracker (SCT), which usually provides eight measurements per track. The barrel pixel layers, which are positioned at radii of 33.3, 50.5, 88.5, and 122.5 mm are of particular relevance to this search. The radial positions of the innermost and outermost SCT barrel layers are 299 mm and 514 mm, respectively. These silicon detectors are complemented by the transition radiation tracker (TRT), which enables radially extended track reconstruction up to $|\eta| = 2.0$. The TRT also provides electron identification information based on the fraction of hits (typically 30 in total) above a higher energy-deposit threshold corresponding to transition radiation.

The calorimeter system covers the pseudorapidity range $|\eta| < 4.9$. Within the region $|\eta| < 3.2$, electromagnetic calorimetry is provided by barrel and endcap high-granularity lead/liquid-argon (LAr) calorimeters, with an additional thin LAr presampler covering $|\eta| < 1.8$ to correct for energy loss in material upstream of the calorimeters. Hadronic calorimetry is provided by the steel/scintillator-tile calorimeter, segmented into three barrel structures within $|\eta| < 1.7$, and two copper/LAr hadronic endcap calorimeters. The solid angle coverage is completed with forward copper/LAr and tungsten/LAr calorimeter modules optimized for electromagnetic and hadronic energy measurements, respectively.

The muon spectrometer (MS) comprises separate trigger and high-precision tracking chambers measuring the deflection of muons in a magnetic field generated by the superconducting air-core toroidal magnets. The field integral of the toroids ranges between 2.0 and 6.0 T m across most of the detector. Three layers of precision chambers, each consisting of layers of monitored drift tubes, cover the region $|\eta| < 2.7$, complemented by cathode-strip chambers in the forward region, where the background is highest. The muon trigger system covers the range $|\eta| < 2.4$ with resistive-plate chambers in the barrel, and thin-gap chambers in the endcap regions.

The luminosity is measured mainly by the LUCID–2 [19] detector that records Cherenkov light produced in the quartz windows of photomultipliers located close to the beampipe.

Events were selected by the first-level trigger system implemented in custom hardware, followed by selections made by algorithms implemented in software in the high-level trigger [20]. The first-level trigger accepted events from the 40 MHz bunch crossings at a rate close to 100 kHz, which the high-level trigger further reduced in order to record complete events to disk at about 1.25 kHz.

A software suite [21] is used in data simulation, in the reconstruction and analysis of real and simulated data, in detector operations, and in the trigger and data acquisition systems of the experiment.

3. Benchmark models

This analysis is motivated by the distinct experimental signature and minimal background associated with the displaced dilepton vertices, rather than by a specific extension of the SM that could produce such a signature. Three models that could produce a leptonically decaying LLP are used as benchmark models to evaluate the sensitivity of the search. All three models contain pair-produced LLPs, but this analysis does not require multiple LLP decays to be reconstructed. The analysis is therefore sensitive to models containing a single LLP.

The first benchmark model ("Z' model") is a simplified model containing a heavy scalar S that decays into a pair of long-lived Z'. A diagram of this process is shown in Fig. 1(a). Prompt decays of a Z' to leptons are heavily constrained [22], but long-lived Z' remain viable. In the simplified model used here the lifetime of the Z' is treated as a free parameter and it is forced to decay into lepton pairs.

The second and third benchmark signal models are both RPV MSSM simplified models where the lightest neutralino $\tilde{\chi}_1^0$ is the lightest supersymmetric particle (LSP). R-parity violation allows the LSP neutralino to decay, possibly with a sufficiently long lifetime to produce a displaced vertex [3]. The two SUSY models implement different production mechanisms of the long-lived neutralino. In both models, the $\tilde{\chi}_1^0$ decays via RPV couplings λ_{121} or λ_{122} [2] into two charged leptons and a neutrino. The λ_{121} coupling results in $ee\nu$ and $e\mu\nu$ decays each with equal branching ratios and the λ_{122} coupling results in $e\mu\nu$ and $\mu\mu\nu$ decays each with equal branching ratios. No requirement on jets, missing transverse momentum, or other leptons is imposed so that the search is as model-independent as possible. The first MSSM model ("Gluino model") implements the pair production of gluinos, where the gluino decays promptly via $\tilde{g} \to qq\tilde{\chi}_1^0$ (Fig. 1(b)). The second MSSM model ("EWkino model") implements electroweakino pair production ($\tilde{\chi}_1^\pm\tilde{\chi}_1^0$, $\tilde{\chi}_1^\pm\tilde{\chi}_2^0$, or $\tilde{\chi}_2^0\tilde{\chi}_1^0$), an example of which is shown in Fig. 1(c). The charginos and neutralinos are assumed to be pure higgsino-like and are nearly mass degenerate, with a 1 GeV mass splitting between the lightest neutralino and both the chargino and heavier neutralino. If a $\tilde{\chi}_1^\pm$ or $\tilde{\chi}_2^0$ is produced, it decays promptly via $\tilde{\chi} \to ff\tilde{\chi}_1^0$, where f is any kinematically allowed fermion.

4. Data and simulated events

The data used in this analysis were collected from pp collisions at $\sqrt{s} = 13$ TeV during Run 2 (2015–2018), corresponding to an integrated luminosity of 140.1±1.2 fb^{-1} [23]. All backgrounds are estimated using collision data. A selection of muon and electron events from the same

[1] ATLAS uses a right-handed coordinate system with its origin at the nominal interaction point (IP) in the centre of the detector and the z-axis along the beam pipe. The x-axis points from the IP to the centre of the LHC ring, and the y-axis points upwards. Polar coordinates (r, ϕ) are used in the transverse plane, ϕ being the azimuthal angle around the z-axis. The pseudorapidity is defined in terms of the polar angle θ as $\eta = -\ln\tan(\theta/2)$ and is equal to the rapidity $y = \frac{1}{2}\ln\left(\frac{E+p_z}{E-p_z}\right)$ in the relativistic limit. Angular distance is measured in units of $\Delta R \equiv \sqrt{(\Delta y)^2 + (\Delta\phi)^2}$.

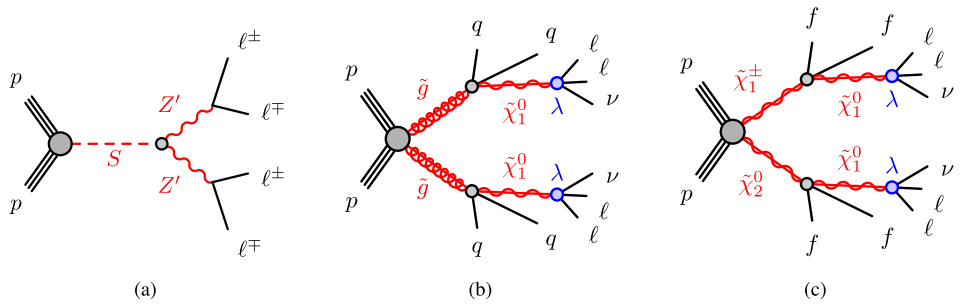

Fig. 1. Diagrams for (a) a pair of Z' produced via a scalar and for a pair of $\tilde{\chi}_1^0$, each produced via (b) a gluino or (c) an electroweakino. For the benchmark models used, the Z' and $\tilde{\chi}_1^0$ are the LLPs while the scalars, gluinos, and higher-mass electroweakinos ($\tilde{\chi}_1^\pm$ and $\tilde{\chi}_2^0$) decay promptly. The symbol λ represents a RPV coupling as described in the text.

data were used for calculating corrections to the Monte Carlo (MC) modeling of lepton efficiencies and their associated systematic uncertainties.

The matrix element (ME) calculations for the Z' model are performed at next-to-leading-order (NLO) by MadGraph 2.6.7 [24] interfaced with Pythia 8.244 [25] using the A14 set of tuned parameters [26] with the NNPDF3.0nlo set of parton distribution functions (PDF) [27]. Signal MC samples are produced for scalar masses from 500 GeV to 1.5 TeV, several Z' masses ranging from 100 to 700 GeV depending on the scalar mass, and Z' mean proper lifetimes times speed of light ($c\tau$) of 10, 30, 100, 300, and 1000 mm. The detector response to each simulated event for all simulated samples is modeled by GEANT4 [21,28].

The ME calculations for the Gluino model and the EWkino model samples are performed at leading-order (LO) by MadGraph 2.8.1 [24] interfaced with Pythia 8.244 using the A14 set of tuned parameters with the NNPDF3.0nlo PDF set. The MEs include up to two extra parton emissions. Signal MC samples for the Gluino model are produced for $\tilde{g}$ masses ranging from 1.5 to 2.5 TeV and several $\tilde{\chi}_1^0$ masses. The heaviest $\tilde{\chi}_1^0$ mass used for each $\tilde{g}$ mass is 300 GeV less than the $\tilde{g}$ mass and the lightest is always 100 GeV. Samples for the EWkino model are produced for $\tilde{\chi}_1^0$ masses ranging from 100 GeV to 1.3 TeV. For both models, separate samples are produced for the same five $c\tau$ for the $\tilde{\chi}_1^0$ as were used for the Z'.

The effect of multiple interactions in the same and adjacent bunch crossings (pileup) was modeled by overlaying the simulated hard-scattering event with inelastic pp events generated with Pythia 8.186 [29] using the NNPDF2.3lo PDF set and the A3 set of tuned parameters [30]. Events in the signal MC samples are weighted such that the pileup distribution in MC closely resembles that in data.

A $t\bar{t}$ sample is used for validation of the procedure for estimating the background from DV formed by random track crossing (Section 7) and as a source of K_S used for a systematic study of combined track reconstruction and vertex reconstruction efficiency for LLPs (Section 8). This sample is simulated using Powheg + Pythia 8.230 [25,31] using the A14 set of tuned parameters with the NNPDF3.0nlo PDF set.

Two Z boson MC samples ($Z \to e^+e^-$ and $\mu^+\mu^-$) are also used to compare to data when deriving multiplicative factors to correct for imperfect modeling of electron and muon detection efficiency. These samples are simulated using Powheg + Pythia 8.186 [32] using the AZNLO [33] set of tuned parameters with the CT10 PDF set [34].

5. Object reconstruction

The standard track (ST) reconstruction algorithm reconstructs the trajectories of charged particles (tracks) from hits in the ID. Requirements placed on the transverse (d_0) and longitudinal (z_0) impact parameters limit the reconstruction efficiency of tracks from displaced decays. To mitigate this reduction in efficiency, tracks from a large radius track (LRT) reconstruction algorithm [35] are also used. The LRT algorithm reconstructs tracks using hits that are not associated with any track from ST reconstruction. Relevant differences between the track requirements for the ST and LRT algorithms are compared in Table 1. Of particular note is the relaxation of the requirements for LRT reconstruction on d_0 and z_0, as well as the maximum number of shared silicon modules and the minimum number of unshared silicon hits between two tracks. These loosened requirements increase the reconstruction efficiency for tracks not originating from the primary vertex (PV).

Table 1
Comparison of requirements between the standard track and large radius track reconstruction algorithms [35].

	ST	LRT
Maximum $\lvert d_0\rvert$ [mm]	10	300
Maximum $\lvert z_0\rvert$ [mm]	250	1500
Maximum $\lvert\eta\rvert$	2.7	5
Maximum shared silicon modules	1	2
Minimum unshared silicon hits	6	5
Minimum silicon hits	7	7

The PV reconstruction algorithm [36] reconstructs vertices using tracks that have parameters consistent with originating from the beam collision region in the $x-y$ plane and is therefore not optimized for displaced decays. A dedicated DV reconstruction algorithm is used to reconstruct vertices at large distances from the PV. The algorithm [37] uses tracks to reconstruct DVs within the pixel and SCT subsystems of the ID. All tracks from both the ST and LRT reconstruction algorithms that have $p_T > 1$ GeV, $|d_0| < 300$ mm, and $|z_0| < 1500$ mm are considered for DV reconstruction. No calorimeter or MS information associated with the track is used, and no corrections are made to the tracks based on their lepton association. The reconstruction algorithm begins by forming a prospective vertex from each possible combination of two tracks, using only tracks not included in collision vertices. To reject tracks not originating from a DV, tracks are only included in the DV if they contain no pixel or SCT hits between the DV and the PV and if they have a hit in the first pixel or SCT layer as the track emerges from the DV.[2] Additionally, at least one of the two tracks in the prospective vertex must satisfy $|d_0| > 2$ mm. Vertices with higher track multiplicity are formed by iteratively merging nearby vertices if this improves the goodness of fit of all tracks to the common vertex. Tracks may then be pruned from the merged vertex to further improve the goodness of fit.

Leptons are reconstructed with the standard ATLAS reconstruction algorithms for electrons [38,39] and muons [40]. Calorimeter information is combined with track information from the ST and LRT reconstruction algorithms to reconstruct and identify electrons. In the case when

[2] A dead pixel or disabled module is treated as a "hit" in both cases, i.e. a dead pixel in between the vertex and PV would cause the vertex to be rejected but a dead pixel in the first layer as the track emerges from the DV would satisfy the requirement for a hit.

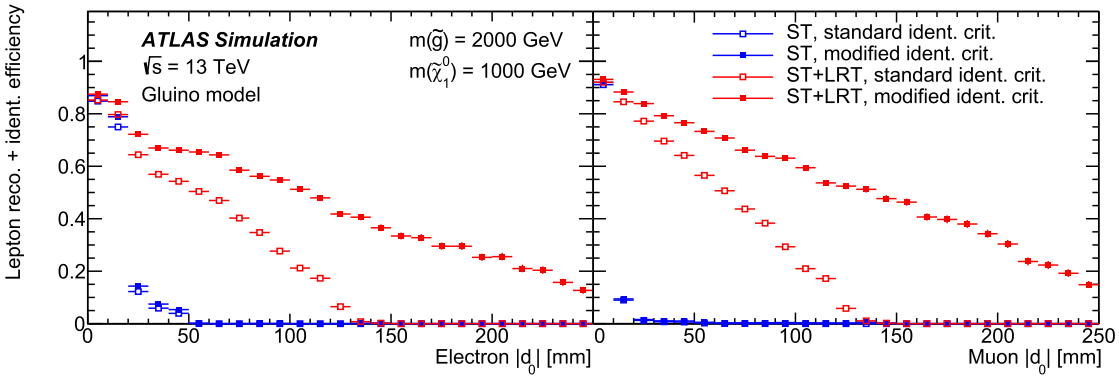

Fig. 2. The efficiency for reconstructing and correctly identifying a simulated lepton from an LLP decay as a function of d_0 for (left) electrons and (right) muons for ST and ST + LRT, with standard and modified working points. The efficiencies were determined using gluino-produced $\tilde{\chi}_1^0$ samples with a $\tilde{g}$ mass of 2000 GeV and a $\tilde{\chi}_1^0$ mass of 1000 GeV, averaged over the five $c\tau$ from 10 to 1000 mm.

several tracks match the same calorimeter energy deposit, the track with the best momentum match to the calorimeter energy is chosen to reconstruct the electron. An additional algorithm [38] refines the parameters of tracks corresponding to electrons, accounting for energy loss due to bremsstrahlung. The refined tracks are not used in the DV reconstruction algorithm or to determine the kinematic properties of the DV, so the updated information is only used in this analysis for identifying the triggering leptons.

Muons must be of the combined type defined in Ref. [40]. Combined muons are reconstructed by pairing tracks reconstructed using only MS information with ID tracks (either reconstructed by the ST or LRT algorithms). A combined fit is then performed using both ID and MS hits and accounting for energy loss in the calorimeters. The combined fitting procedure allows for a reassignment of MS hits based on the combined fit trajectory.

6. Event selection

Events with dilepton DVs are selected via a series of criteria, either applied to the event, the constituent leptons, or the DVs themselves. The event selection begins by selecting collision events with leptons that may be displaced and requiring the presence of a DV. Criteria are then applied to the displaced leptons and their associated DVs to isolate potential signal events.

6.1. Event level selection criteria

Events are required to have a PV with at least two associated tracks. The PV is selected as the pp collision vertex with the largest Σp_{T}^2, the squared transverse momentum of all associated tracks with $p_{\mathrm{T}} > 0.5$ GeV. Additionally, events must be recorded during time periods where detector subsystems were functioning under good operating conditions [41].

Events are selected using triggers that do not rely on ID track information. Track reconstruction algorithms used by the Run-2 triggers do not include an equivalent of the LRT algorithm; therefore, a requirement for the presence of an ID track can suppress trigger efficiency for displaced leptons. The "MS only" muon trigger selects an MS track with $p_{\mathrm{T}} > 60$ GeV and $|\eta| < 1.05$ [42]. For electrons two triggers are used: a single photon trigger and a diphoton trigger [43]. The use of a photon trigger is appropriate to target displaced electrons because electrons and photons leave similar energy deposits in the electromagnetic calorimeter. The single photon trigger requires the reconstructed object satisfy $p_{\mathrm{T}} > 140$ GeV, while the diphoton trigger imposes a softer requirement, $p_{\mathrm{T}} > 50$ GeV, for both objects. No requirement is placed on η for either photon trigger other than the implicit bounds set by the geometry of the electromagnetic calorimeter. The combined trigger efficiency is typically above 80% for all vertex types for decays within the fiducial region. Individually, the electron triggers generally have a higher efficiency than the muon trigger due to their larger pseudorapidity coverage. Events selected by the trigger are required to include a reconstructed lepton which spatially matches the location of the object selected by the trigger. The triggering lepton must also satisfy both $|d_0| > 2$ mm and a requirement on its p_{T} that matches the trigger requirement. If the event was selected by the diphoton trigger, two leptons must satisfy the trigger requirements.

A cosmic veto is applied to suppress cosmic-ray muon background contributions. A cosmic-ray muon may be mis-reconstructed as a pair of back-to-back and oppositely charged muons. Calorimeter deposits resulting from muon bremsstrahlung may also cause a muon to be reconstructed as an electron. Back-to-back tracks can be distinguished by values of $\Delta R_{\cos} = \sqrt{(|\Delta\phi| - \pi)^2 + (\Sigma\eta)^2}$ that are close to zero, where $\Sigma\eta = \eta_1 + \eta_2$ and $\Delta\phi = \phi_1 - \phi_2$ for the η and ϕ of the two tracks. Imposing the requirement $\Delta R_{\cos} > 0.01$ on all $\mu\mu$ pairs and μe pairs in the event effectively eliminates these cosmic-ray muon events. The number of signal events eliminated by the cosmic veto does not exceed 1%.

6.2. Lepton selection criteria

To qualify as signal electrons, reconstructed electrons must satisfy the VeryLooseLLH identification requirements defined in ref. [38] but with requirements on d_0 and on the number of pixel hits associated with the track removed. Signal muons must satisfy the Loose identification requirements defined in ref. [40] but with the requirements on the number of pixel hits associated to the track removed. Fig. 2 shows the efficiency for an electron or a muon from an LLP decay in a benchmark sample to be both reconstructed and satisfy lepton identification criteria. The efficiencies are shown using only the ST reconstruction algorithm versus both ST and LRT, and the standard versus modified lepton identification criteria. Including the LRT and modified identification criteria greatly improves the efficiency. Multiplicative factors to correct for the mismodeling of lepton identification and triggering efficiencies in signal samples are also applied, as discussed in Section 8. An overlap removal to remove ambiguity between electrons, muons, and jets is applied similar to that described in ref. [44], with the exception that the ΔR requirement between electrons and muons is not applied to allow for more highly collimated signal leptons.

Some analysis requirements are applied to the lepton's kinematic parameters, while others are applied to the kinematic parameters of the ID track, which may be different. The use of ID track parameters, which are those available to the DV reconstruction algorithm, simplifies the calculation of systematic uncertainties. The kinematic parameters of the ID track are used for the baseline track requirements $p_{\mathrm{T}} > 10$ *GeV* for both lepton flavors and $|\eta| < 2.47$ (2.5) for electrons (muons). The kinematic

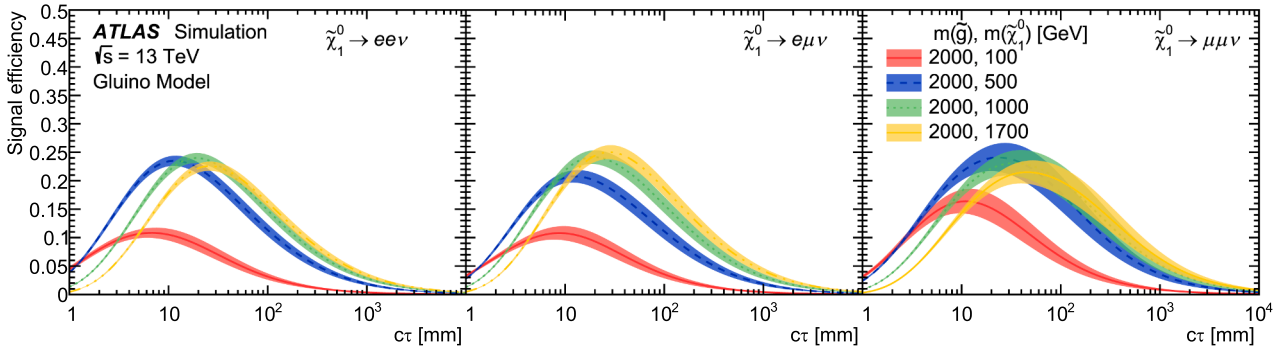

Fig. 3. Total signal efficiency for an LLP decay as a function of $c\tau$ for the gluino-produced $\tilde{\chi}_1^0$ with a $\tilde{g}$ mass of 2000 GeV and $\tilde{\chi}_1^0$ mass of 100, 500, 1000, or 1700 GeV decaying into (left) $ee\nu$, (middle) $e\mu\nu$, and (right) $\mu\mu\nu$ final states. The colored bands represent the total uncertainty at one standard deviation.

parameters of the leptons themselves are used for lepton identification, charge requirements, the cosmic veto, and trigger matching, the last of which is discussed in Section 6.3.

The combined fit of the muon track based on both ID and MS hits must satisfy $\chi^2/\text{dof} < 10$. The displaced decay of a charged hadron to a muon may be incorrectly reconstructed as a combined muon if the ID track from the hadron is matched to the MS track of the muon by the reconstruction software. In such cases, the ID and MS components are often poorly aligned, so the requirement on χ^2 effectively removes most muons originating from charged hadron decays with negligible impact on signal muons in benchmark samples.

6.3. Displaced vertex selection criteria

To suppress background, signal DVs must have transverse displacement from the PV satisfying $R_{xy} = \sqrt{(x_{\text{DV}} - x_{\text{PV}})^2 + (y_{\text{DV}} - y_{\text{PV}})^2} > 2$ mm. The DV must also satisfy $\sqrt{(x_{\text{DV}})^2 + (y_{\text{DV}})^2} < 300$ mm and $|z_{\text{DV}}| < 300$ mm (both measured relative to the ATLAS detector origin), defining a fiducial region in the barrel of the ID bounded by the innermost SCT layer. DVs are rejected if they are within disabled pixel modules [45]. A separate "material veto" [46], designed to suppress displaced vertices from photon conversions, is applied to DVs that contain an electron and are within the tracking layers or the support structures. Following the strategy used in previous ATLAS DV analyses [47–49], DVs are required to be reconstructed with $\chi^2/\text{dof} < 5$. An event is permitted to contain more than one signal DV.

At least two of the ID tracks in the DV must be associated with oppositely charged leptons that satisfy the modified identification criteria discussed in Section 6.2. One of the leptons in a DV must be the lepton selected by the trigger (both leptons in the case of the diphoton trigger) and satisfy the stricter kinematic requirements discussed in Section 6.1. Finally, the invariant mass of the ID tracks of the lepton pair forming the DV must satisfy $m_{\text{DV}} > 12$ GeV to suppress backgrounds from SM particles. To allow reinterpretation using other models, additional tracks (including leptonic tracks) are permitted in the DV despite not being expected in the benchmark models. Enforcing a requirement of exactly two leptonic tracks in a DV would remove < 1% of signal vertices in the benchmark models. In the case of a DV containing three or more leptonic tracks, each pair of tracks is treated as a potential signal DV, with separate trigger matching and mass requirements for each track pair.

Fig. 3 shows an example of the efficiency for a $\tilde{\chi}_1^0$ decay to satisfy the full selection criteria as a function of $c\tau$. The uncertainty band represents the total uncertainty at one standard deviation, including the sources of systematic uncertainty discussed in Section 8. The extrapolation to lifetimes other than those of the generated samples is discussed in Section 9. The trigger efficiency for dimuon vertices is lower than that for vertices with electrons, but its impact on the total dimuon efficiency is mitigated by the higher reconstruction efficiency for displaced muons previously shown in Fig. 2. For the same parent mass, the peak efficiency for higher LLP masses occurs at larger proper lifetimes due to the lower boost of the LLP. A highly boosted LLP, such as in the case of the 100 GeV $\tilde{\chi}_1^0$ and 2000 GeV $\tilde{g}$, can produce highly collimated daughters, resulting in the reconstruction of only one lepton and hence lower signal efficiency. The efficiencies and systematic uncertainties are presented per LLP decay for each vertex type; however, all benchmark samples contain two LLPs and hence limits are evaluated in Section 9 assuming two decays per event.

It is of particular interest to compare the reconstruction efficiency shown in Fig. 3 with that obtained by ATLAS for displaced dimuon vertices reconstructed using standalone muons [10], i.e. muons reconstructed using MS information only. While the two analyses probe different RPV SUSY models, the comparison nevertheless provides useful context on the complementarity of ID and MS displaced vertex searches. When using standalone muons, the efficiency for events containing a pair of long-lived $\tilde{\chi}_1^0$ (each with $m(\tilde{\chi}_1^0) = 1000$ GeV) peaks at ~10% at a $c\tau$ of 1000 mm. The current analysis, which includes ID tracks and uses a more sophisticated DV reconstruction algorithm, reaches a higher peak efficiency at lower $c\tau$. When considering a same-mass $\tilde{\chi}_1^0$ and only considering a single decay into a muon pair, this analysis achieves an efficiency that peaks at ~23% at a $c\tau$ of 34 mm and yields only a somewhat lower value of ~6% at 1000 mm.

7. Background estimate

The background from decays of SM particles produced by proton–proton collisions is reduced to negligible levels by requirements on the invariant mass of the signal lepton pair forming the DV and the transverse displacement of the DV relative to the PV. Two additional sources of background are considered: DVs resulting from cosmic-ray muons and from randomly crossing lepton tracks.

The dimuon cosmic-ray background is estimated in a control region of dimuon DVs satisfying all signal requirements except for the cosmic veto, which is inverted. The tail of the $\Delta R_{\cos}$ distribution of dimuon DVs in this region ($\Delta R_{\cos} < 0.01$) is fit to an exponential distribution and extrapolated into the signal region ($\Delta R_{\cos} > 0.01$). The fit range, which starts at $\Delta R_{\cos} = 0.0027$, is chosen to produce the best agreement between the prediction and observed DVs in the region $0.005 < \Delta R_{\cos} < 0.01$, adjacent to the signal region. The extrapolation yields an estimated cosmic background of $(8.3 \pm 6.0) \times 10^{-3}$ $\mu^+\mu^-$ events, where the uncertainty is statistical.

One of the two reconstructed muon tracks from a cosmic-ray muon may fail to satisfy the muon signal requirements while satisfying the electron signal requirements due to bremsstrahlung by the muon, so the cosmic veto is also applied to electron-muon pairs. A similar extrapolation method cannot be used to estimate a cosmic background in the $e^\pm\mu^\mp$ signal region because there are only two $e^\pm\mu^\mp$ events with $\Delta R_{\cos} < 0.01$. The $\Delta R_{\cos}$ distribution is instead assumed to be similar to that of $\mu^+\mu^-$ events but suppressed by a factor equal to the ratio of the statistics of the

two control regions. The dimuon cosmic background is thus scaled down to yield an estimated background of $(1.2 \pm 0.9) \times 10^{-5}$ $e^{\pm}\mu^{\mp}$ vertices in the signal region, where the uncertainty is statistical.

The background from two randomly crossing lepton tracks forming a signal DV is estimated from data by using large numbers ($10^6 - 10^8$, depending on the channel) of toy "mixed" events. Each toy event consists of two randomly selected leptons (which satisfy all signal lepton requirements) from different data events with a randomly selected PV from a third event. The lepton pair is only considered a "candidate pair" if it has the necessary kinematics to be selected by one of the triggers, the leptons have opposite-sign charges, and the invariant mass of the leptons is greater than 12 GeV. The lepton tracks are shifted spatially around the new PV to preserve the impact parameters relative to the PV in their original events. Due to computational limitations, these tracks retain their pattern of hits in each layer even if the shifting would result in a different expected hit pattern. DV reconstruction is then run on each toy event and, if a DV is successfully reconstructed, the analysis requirements are applied to the DV. This method yields the probability for a signal DV to be produced from two randomly crossing leptonic tracks. This probability can then be applied to the number of candidate lepton pairs in the data. Candidate pairs in data include any pairs of ID tracks in the same event that satisfy the same criteria used in toy selection.

Multiple validations of the event-mixing process were performed on signal MC, non-signal MC ($t\bar{t}$), and data. The spatial shifting of tracks was validated by shifting all tracks in an MC signal event around a randomly selected PV and rerunning the vertex reconstruction algorithm. The overall difference between the number of reconstructed signal DVs due to shifting tracks is 1.1%. There is a loss of ∼3 % of signal DVs, but a gain of ∼2% of signal DVs that previously were not reconstructed, yielding a net loss of 1.1%. A vertex that originally failed to satisfy the selection criteria because it was in a disabled module but was "shifted" out may now satisfy the criteria, while vertices can be lost to the same effect. The largest effect is due to rejecting individual tracks due to differences between the expected patterns of hits in the silicon layers. For example, a track that originally intersects with a dead pixel in the next layer outside the DV (thus fulfilling the DV reconstruction algorithm requirements) will lack the expected hit if moved into a region without an adjacent dead pixel, resulting in rejection by the DV reconstruction algorithm. The predictive ability of the method was tested using non-leptonic tracks (see Section 8), which is used to set a systematic uncertainty.

There are 6646 e^+e^-, 792 $e^{\pm}\mu^{\mp}$, and 3134 $\mu^+\mu^-$ candidate pairs observed in data, and at least 10^3 times more toy candidate pairs were generated for each vertex type. None of the reconstructed dilepton DVs in the toy events satisfied all signal requirements. The upper limit (at 95% confidence) of the probability of randomly crossing leptons producing a signal DV is $\mathcal{O}(10^{-6})$ for each of e^+e^-, $e^{\pm}\mu^{\mp}$, and $\mu^+\mu^-$. Rather than using a fixed probability, the numbers of toy and observed candidate pairs are treated as control and signal regions respectively when setting limits on signal cross-sections, allowing for the probability to be fit simultaneously with the signal strength. The procedure for determining the limits is detailed in Section 9.

8. Systematic uncertainties

The dominant source of systematic uncertainty in the signal efficiency is the modeling of track and DV reconstruction. This uncertainty is estimated from a sample of $K_S \to \pi^+\pi^-$ reconstructed in MC and data. Due to the relatively low mass and p_{T} of the K_S, few of the signal requirements can be applied beyond the standard vertex quality requirements. Instead, to select K_S, the DVs are required to have exactly two oppositely charged-particle tracks, 470 MeV $< m_{\pi\pi} <$ 530 MeV, $R_{xy} > 15$ mm, and tracks with longitudinal separation $|\Delta z_0| < 2$ mm. The number of reconstructed K_S vertices is binned in R_{xy} after reweighting the simulated events such that the p_{T} spectrum of the K_S in the MC reproduces that in the data. The vertices are categorized based on the algorithms that reconstructed the two tracks from the K_S decay (ST/ST, ST/LRT, and LRT/LRT) with separate systematic uncertainties calculated for each category. A common normalization for the three categories is used by normalizing the number of ST/ST vertices at low R_{xy} in the MC to the data, where modeling is best understood for both track and vertex reconstruction. The residual discrepancy between MC and data in each bin is taken as the systematic uncertainty. Some variation is observed in the agreement between data and MC based on the year and corresponding MC sample considered. Consequently, a separate normalization factor and systematic uncertainty is calculated for each year. The systematic uncertainty is generally less than 20% per vertex at low and moderate R_{xy}, but at high R_{xy} it can be up to 34% for ST/ST vertices, 40% for ST/LRT vertices, and 44% for LRT/LRT vertices.

Using the residual discrepancy between MC and data as the systematic uncertainty for reconstructing a DV results in a conservative estimate in comparison to decomposing the uncertainty into a correlated and uncorrelated component relative to the reconstruction of the two tracks. Inefficiencies in K_S reconstruction may result from the failure to reconstruct individual tracks due to effects such as multiple scatterings, or from a failure to reconstruct both tracks such as when the particle decays within a dead Si module. The former is uncorrelated between tracks, while the latter is an example of a fully correlated effect. The residual discrepancy may be converted into uncorrelated, per-track uncertainties and propagated through to vertices [48,50], which will yield a smaller uncertainty for the vertex. Possible correlations can then be estimated via expanded studies of the geometric or time dependence of the data/MC ratio. The statistical analysis discussed in Section 9 does not have a strong dependence on this dominant uncertainty; therefore the simpler but conservative method that assumes full correlation is used.

Highly boosted and collimated lepton pairs may have a small d_0 even when the R_{xy} of their DV is large, resulting in a significant proportion of displaced ST/ST and ST/LRT vertices for some mass points. The systematic uncertainty is therefore calculated separately for each mass hypothesis. Fig. 4 shows the extrapolated average systematic uncertainties per vertex for a benchmark sample as a function of $c\tau$. The systematic uncertainty increases at higher $c\tau$ due to the increasing presence of LRT tracks. The reconstruction efficiency for muons with LRT tracks is higher than that for electrons with LRT tracks as shown in Fig. 2. Consequently, at large $c\tau$, where more LRT tracks are produced, both the average efficiency (Fig. 3) and the average systematic uncertainty (Fig. 4) are higher for muons than for electrons.

Custom multiplicative factors are calculated as a function of lepton kinematics to correct MC lepton distributions for the imperfect modeling of the efficiency of the triggers and lepton identification working points. The factors are calculated using a tag-and-probe method similar to that described in ATLAS Collaboration [39] based on $Z \to \ell^+\ell^-$ events in data and MC. The multiplicative factors for electron triggering and identification are approximately 1, except in the transition region between the barrel and endcap calorimeters ($1.37 < |\eta| < 1.52$) where values for triggering generally range from 0.90 to 1.02 and values for identification range from 0.98 to 1.02. For muon identification, values are likewise approximately 1 except in the central η region, where they can be as low as 0.98. For triggering on muons, the multiplicative factors typically range from 0.7 to 1.0. The factors have an associated uncertainty that is propagated through the analysis by shifting the factors upwards and downwards by their associated systematic uncertainty. The final systematic uncertainties associated with the triggers and lepton identification are both approximately 1% or smaller. The theory uncertainties associated with modeling the benchmark signal samples are the uncertainty in the cross-section, the PDF uncertainties, the uncertainties in the factorization and renormalization scales, and the uncertainty associated with initial-state and final-state radiation combined with multiple parton interactions (ISR/FSR/MPI). The methods used follow those described in ref. [51]. The largest of these uncertainties are the PDF uncertainties, at 5.2%, followed by the ISR/FSR/MPI uncertainty at 3.0%. These values

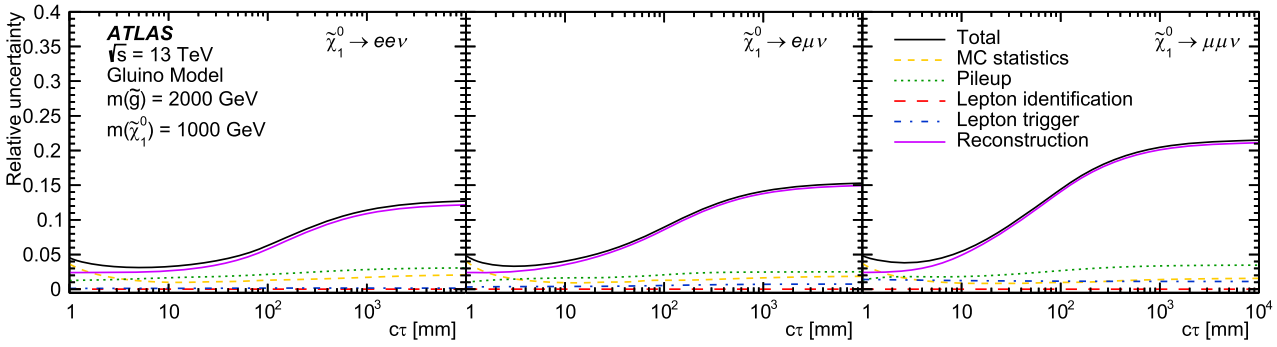

Fig. 4. Systematic uncertainties in the signal DV selection efficiency extrapolated as a function of $c\tau$ for the gluino-produced $\tilde{\chi}_1^0$ with a $\tilde{g}$ mass of 2000 GeV and $\tilde{\chi}_1^0$ mass of 1000 GeV decaying into (left) $ee\nu$, (middle) $e\mu\nu$, and (right) $\mu\mu\nu$ final states.

are significantly smaller than the dominant sources of systematic uncertainties so the largest value calculated amongst the samples is applied to all signal samples as a constant value.

The systematic uncertainty associated with the random track crossing background is calculated using ID tracks not identified as leptons but satisfying all other signal requirements. Due to computational limitations, shifted tracks retain their original set of hits in the ID tracking layers, even if the shift would result in a different expected hit pattern. The systematic impact from this is inherently included in the systematic uncertainty determined from comparing observed and predicted number of non-leptonic vertices. The DV mass and R_{xy} distributions observed in data are well reproduced by the DVs created from toy events. The probability of randomly crossing non-leptonic tracks to form a signal DV is calculated to be $(3.07 \pm 0.09) \times 10^{-7}$. That probability is applied to the observed number of non-leptonic track candidate pairs in data (4.22×10^{11}) to yield the predicted number of non-leptonic DVs in data of 143800 ± 4200. The observed number of non-leptonic DVs is 126210. The difference between the expectation and observation is combined in quadrature with the statistical uncertainty to yield a systematic uncertainty of 14%.

The systematic uncertainty associated with the procedure of fitting an exponential fit function to the cosmic background histogram is estimated by varying the histogram bin width and varying the lower bound of the fit range. The two contributions are combined in quadrature to yield a systematic uncertainty of 44%.

The uncertainty in the combined 2015–2018 integrated luminosity is 0.83% [23], obtained using the LUCID-2 detector [19] for the primary luminosity measurements, complemented by measurements using the inner detector and calorimeters. The uncertainty associated with the pileup weighting procedure was evaluated by applying alternate weight sets and found to increase with higher $c\tau$, while remaining subdominant.

Finally, the uncertainty associated with the lifetime extrapolation procedure described below was calculated by comparing the deviation of nominal efficiencies to extrapolated values. A 2.0% uncertainty is conservatively assigned to the signal DV selection efficiency.

9. Results

No events are observed in the signal region, which is consistent with the background expectation. The analysis is a cut-and-count analysis, allowing limits to be set for each benchmark model using a single bin counting experiment. Therefore, limits are set at the 95% confidence level using the CLs method [52] based on RooStats [53] via a toys-based method with 25,000 pseudo-experiments. The signal region includes both the observed number of events (zero), the expected number of signal events for each benchmark model, and the cosmic-ray muon background estimates for $\mu\mu$ and $e\mu$ vertices. Additionally, the numbers of candidate track pairs discussed in Section 7 is included. Three control regions, one for each vertex type, are defined to include the number of candidate pair toy events created and the number of signal vertices created in the toy events (zero). While performing the fit to observed data, both the signal strength and the probability of producing a signal vertex from randomly crossing track pairs can be scaled, allowing for the possibility of non-zero probabilities despite the lack of toy DVs in the signal region. Due to the lack of observed events after unblinding, the fitted probabilities are generally $O(10^{-10})$, with an error several orders of magnitude larger than the central values. When accounting for the error, the order of magnitude is comparable to but does not exceed the calculated upper limit on the crossing probability of $O(10^{-6})$ discussed in Section 7.

Limits are set separately for each decay channel as a function of $c\tau$, utilizing a lifetime reweighting procedure applied to signal efficiencies. The lifetime reweighting procedure extrapolates the acceptance times efficiency of the finite number of signal samples generated with specific $c\tau$ to a continuous distribution. Weights are applied to each LLP decay vertex corresponding to the relative frequency of decays at the lifetime of that individual particle as a function of the generated and target sample $c\tau$. More details can be found in ref. [9].

Only one LLP decay must be detected for the event to qualify as a signal event. The production of two LLPs per event in the benchmark models studied increases the probability that at least one signal vertex is found. For the Z' benchmark samples the limits are presented at event-level, assuming both Z' decay into the same vertex type (e^+e^-, $e^\pm\mu^\mp$, or $\mu^+\mu^-$). For the SUSY models the limits are interpreted assuming a coupling of $\lambda_{121} \neq 0$ or $\lambda_{122} \neq 0$ (with all other $\lambda_{ijk} = 0$), resulting in decays into ee and $e\mu$ in the former case and $e\mu$ and $\mu\mu$ in the latter. Extracted limits are shown together with the theory cross-section for the SUSY models. Theory signal cross-sections for the Gluino model are calculated to approximate next-to-next-to-leading order in the strong coupling constant, adding the resummation of soft gluon emission at next-to-next-to-leading-logarithmic accuracy (approximate NNLO + NNLL) [54–61]. The nominal cross-section and the uncertainty are derived using the PDF4LHC15_mc PDF set, following the recommendations of ref. [62]. Theory signal cross-sections for the EWkino model are calculated to next-to-leading order in the strong coupling constant, adding the resummation of soft gluon emission at next-to-leading-logarithmic accuracy (NLO + NLL) [63–67]. The nominal cross-section and the uncertainty are taken from an envelope of cross-section predictions using different PDF sets and factorization and renormalization scales, as described in ref. [51].

Observed and expected limits on the Z' production cross-section times branching ratio as a function of lifetime are shown in Fig. 5 for $m_S = 1000$ GeV. Both the observed and expected limits are plotted, but the lines overlap due to the agreement between the background prediction and observation. At longer Z' lifetimes, weaker limits are set on lighter Z' for the same scalar mass because the more highly boosted Z' results in more decays outside of the ID. Conversely, at shorter

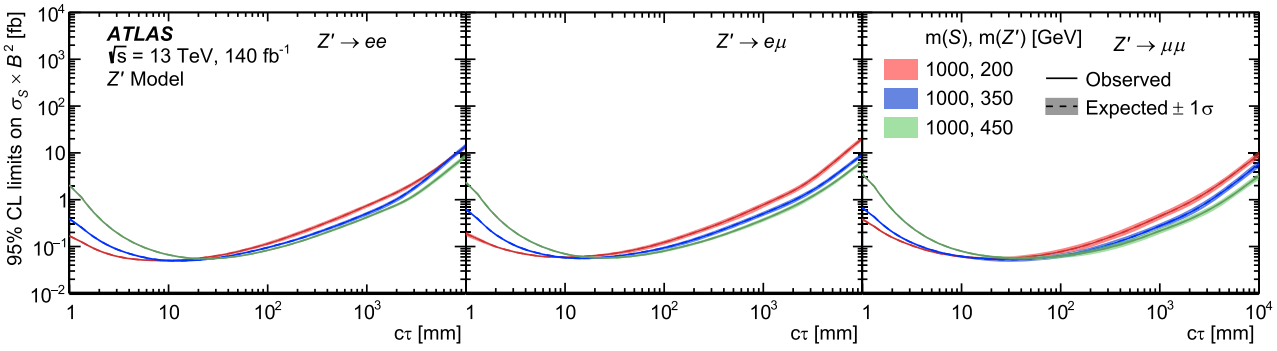

Fig. 5. Observed and expected limits on the product of cross-section and B^2 as a function of $c\tau$ for models with an S mass of 1000 GeV and Z' masses between 200 and 450 GeV decaying into (left) e^+e^-, (middle) $e^\pm\mu^\mp$, and (right) $\mu^+\mu^-$ final states. The branching ratio B is assumed to be 100% to the given final state for both Z'.

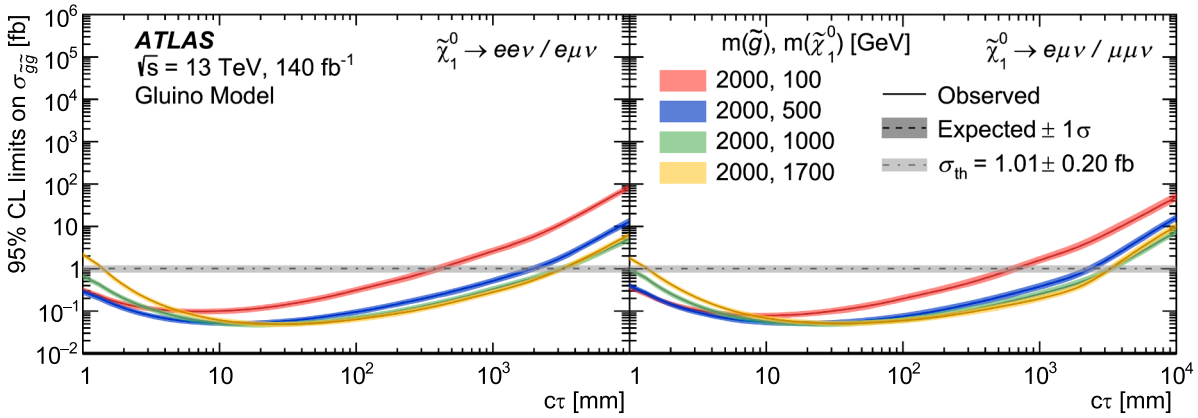

Fig. 6. Observed and expected limits on the signal production cross-section as a function of $c\tau$ for the gluino-produced $\tilde{\chi}_1^0$ with a $\tilde{g}$ mass of 2000 GeV and $\tilde{\chi}_1^0$ masses of 100, 500, 1000, and 1700 GeV with the $\tilde{\chi}_1^0$ decaying with equal branching ratios to (left) $ee\nu$ and $e\mu\nu$ and to (right) $e\mu\nu$ and $\mu\mu\nu$. These scenarios correspond to RPV couplings (left) $\lambda_{121} \neq 0$ or (right) $\lambda_{122} \neq 0$ with all other λ_{ijk} assumed to be zero. The dashed horizontal line represents the theory production cross-section (σ_{th}).

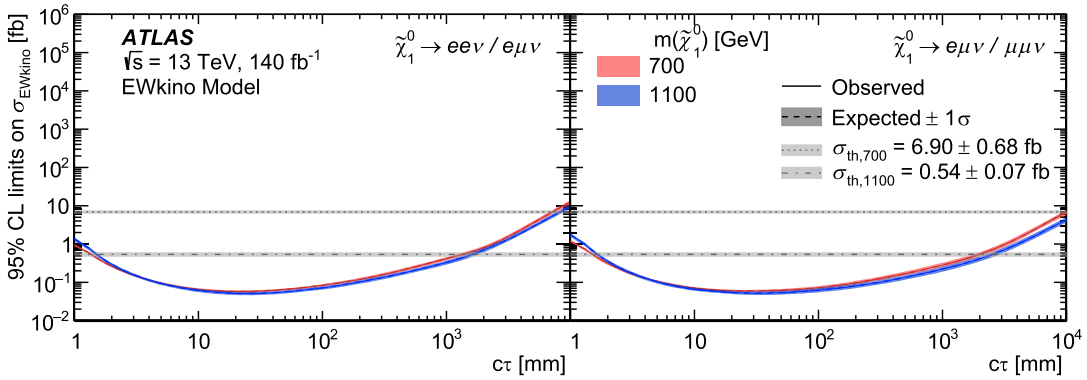

Fig. 7. Observed and expected limits on the signal production cross-section as a function of $c\tau$ for the electroweakino-produced $\tilde{\chi}_1^0$ with masses of 700 and 1100 GeV with the $\tilde{\chi}_1^0$ decaying with equal branching ratios to (left) $ee\nu$ and $e\mu\nu$ and to (right) $e\mu\nu$ and $\mu\mu\nu$. These scenarios correspond to RPV couplings (left) $\lambda_{121} \neq 0$ or (right) $\lambda_{122} \neq 0$ with all other λ_{ijk} assumed to be zero. The dashed horizontal lines represent the theory production cross-sections (σ_{th}).

lifetimes the limits are weaker for heavier Z' because the less-boosted particles will often decay before reaching the ID. The upper limits for different scalar masses are similar with stronger limits set for higher scalar masses due to the higher reconstruction efficiency. For example, the upper limits for the $e\mu$ channel at 10 mm (near the peak efficiencies) are 0.1120, 0.0589, and 0.0534 fb for $(m_S, m_{Z'})$ = (500, 200) GeV, (1000, 200) GeV, and (1500, 250) GeV respectively. The larger error bands for dimuon vertices are a result of the larger track and DV reconstruction systematic uncertainty for these vertices, as discussed in Section 8.

Observed and expected limits on the gluino-produced $\tilde{\chi}_1^0$ signal cross-section as a function of $c\tau$ are shown in Fig. 6 for $m(\tilde{g})$ = 2000 GeV. As in the case of the Z' model limits, the lines for the observed and expected limits overlap in both SUSY models. For the same $\tilde{g}$ mass, more stringent limits are set at long lifetimes for heavier $\tilde{\chi}_1^0$ masses and at shorter lifetimes for lighter $\tilde{\chi}_1^0$ masses—the same parent-daughter trend observed for the Z' samples. For $m(\tilde{g})$ = 2000 GeV, the largest excluded $c\tau$ in the λ_{121} (λ_{122}) channel ranges from 400 mm (660 mm) for $m(\tilde{\chi}_1^0)$ = 100 GeV up to 3200 mm (3300 mm) for $m(\tilde{\chi}_1^0)$ = 1000 GeV. The smallest lifetime excluded is the 1 mm lower bound of the range investigated in

this analysis for all $\tilde{\chi}_1^0$ masses except for $m(\tilde{\chi}_1^0) = 1700$ GeV, which is only excluded down to ~1.5 mm in both channels. For the higher mass $m(\tilde{g}) = 2500$ GeV, a narrower range of lifetimes is excluded, with no exclusion for $m(\tilde{\chi}_1^0) = 100$ GeV. For λ_{121}, the excluded $c\tau$ range for a $\tilde{\chi}_1^0$ with a mass of 500, 1000, or 2200 GeV is between 2.8 and 63 mm, 4.0 and 100 mm, and 7.8 and 150 mm, respectively. In the case of λ_{122}, the excluded $c\tau$ range for a $\tilde{\chi}_1^0$ with a mass of 500, 1000, or 2200 GeV is between 3.7 and 92 mm, 4.9 and 150 mm, and 9.1 and 200 mm, respectively. By contrast, for the lowest gluino mass ($m(\tilde{g}) = 1500$ GeV) and in both channels, all $c\tau$ between 1 and 10 000 mm are excluded for all $\tilde{\chi}_1^0$ masses except for 100 GeV, where the largest excluded lifetime is at 3900 mm (5400 mm) for the λ_{121} (λ_{122}) channel.

Observed and expected limits on an electroweakino-produced $\tilde{\chi}_1^0$ signal cross-section as a function of lifetime are shown in Fig. 7 for $m(\tilde{\chi}_1^0) = 700$ GeV and $m(\tilde{\chi}_1^0) = 1100$ GeV. For $m(\tilde{\chi}_1^0) = 1100$ GeV, $c\tau$ are excluded with a lower bound of 1.5 mm (1.7 mm) and upper bound of 1600 mm (2600 mm) for the λ_{121} (λ_{122}) channel. Limits are more modest for $m(\tilde{\chi}_1^0) = 1300$ GeV, ranging between about 3.1 mm (3.6 mm) for the lower bound and 460 mm (660 mm) for the upper bound for the $\lambda_{121} \neq 0$ ($\lambda_{122} \neq 0$) channel. For $m(\tilde{\chi}_1^0) = 900$ GeV and $m(\tilde{\chi}_1^0) = 700$ GeV the lower bound of the limit on $c\tau$ is at 1 mm, the lower bound of the investigated range. In the case of $m(\tilde{\chi}_1^0) = 900$ GeV the excluded $c\tau$ range extends to 3300 mm (5200 mm) for the λ_{121} (λ_{122}) channel, while for $m(\tilde{\chi}_1^0) = 700$ GeV the range extends to a larger 7200 mm for λ_{121} and to the edge of the evaluated range for λ_{122}. For $m(\tilde{\chi}_1^0) = 500$ GeV and lighter, the full range of considered $c\tau$ is excluded.

10. Conclusion

A search for long-lived neutral particles decaying into pairs of leptons was performed using data collected with the ATLAS detector at the LHC. This is the first analysis to search for heavy LLP decays into displaced dilepton vertices using the full Run-2 pp data. Previous searches by the ATLAS and CMS Collaborations focused on lighter LLPs (usually decaying into dimuon pairs) or used partial Run-2 data. No previous analysis, other than the ATLAS search using similar reconstruction and selection criteria [9] but less than one third of the data, has searched for all three signatures (ee, $e\mu$, and $\mu\mu$ DVs).

No events were observed in the signal region, which is consistent with background expectations. These results complement the previous search based on 32.8 fb^{-1} of pp data [9] interpreted using different models. The search yields new limits on the cross-section for the production of a scalar that decays into a pair of long-lived Z', both decaying into the same final state (e^+e^-, $e^\pm\mu^\mp$, or $\mu^+\mu^-$), with $c\tau$ from 1 to 10 000 mm. The extracted limits are for a scalar with mass of 0.5 to 1.5 TeV and Z' with mass of 100 to 700 GeV. The search also excludes the production of a long-lived neutralino $\tilde{\chi}_1^0$ that decays through a λ_{121} or λ_{122} coupling into two leptons and a neutrino in a similar lifetime range. From the pair production of gluinos with mass of 1.5 to 2.0 TeV, $\tilde{\chi}_1^0$ with mass of 0.1 to 1.7 TeV are excluded at most $c\tau$ from 1 to 10 000 mm. For $\tilde{\chi}_1^0$ produced directly or in the decay of $\tilde{\chi}_2^0$ or $\tilde{\chi}_1^\pm$, neutralinos with mass of 0.1 to 0.5 TeV are excluded for all lifetimes in the considered range, with smaller lifetime ranges excluded for $\tilde{\chi}_1^0$ masses increasing from 0.7 to 1.3 TeV. These are the first limits set on high mass, long-lived neutralino models using gluino and electroweakino production modes with decays into lepton pairs, with the exception of gluino-produced neutralino decays into muons [10].

Data availability

The data for this manuscript are not available. The values in the plots and tables associated to this article are stored in HEPDATA (http://hepdata.cedar.ac.uk).

Declaration of competing interest

The authors declare that they have no known competing financial interests or personal relationships that could have appeared to influence the work reported in this paper.

Acknowledgments

We thank CERN for the very successful operation of the LHC and its injectors, as well as the support staff at CERN and at our institutions worldwide without whom ATLAS could not be operated efficiently.

The crucial computing support from all WLCG partners is acknowledged gratefully, in particular from CERN, the ATLAS Tier-1 facilities at TRIUMF/SFU (Canada), NDGF (Denmark, Norway, Sweden), CC-IN2P3 (France), KIT/GridKA (Germany), INFN-CNAF (Italy), NL-T1 (Netherlands), PIC (Spain), RAL (UK) and BNL (USA), the Tier-2 facilities worldwide and large non-WLCG resource providers. Major contributors of computing resources are listed in ref. [68].

We gratefully acknowledge the support of ANPCyT, Argentina; YerPhI, Armenia; ARC, Australia; BMWFW and FWF, Austria; ANAS, Azerbaijan; CNPq and FAPESP, Brazil; NSERC, NRC and CFI, Canada; CERN; ANID, Chile; CAS, MOST and NSFC, China; Minciencias, Colombia; MEYS CR, Czech Republic; DNRF and DNSRC, Denmark; IN2P3-CNRS and CEA-DRF/IRFU, France; SRNSFG, Georgia; BMFTR, HGF and MPG, Germany; GSRI, Greece; RGC and Hong Kong SAR, China; ICHEP and Academy of Sciences and Humanities, Israel; INFN, Italy; MEXT and JSPS, Japan; CNRST, Morocco; NWO, Netherlands; RCN, Norway; MNiSW, Poland; FCT, Portugal; MNE/IFA, Romania; MSTDI, Serbia; MSSR, Slovakia; ARIS and MVZI, Slovenia; DSI/NRF, South Africa; MICIU/AEI, Spain; SRC and Wallenberg Foundation, Sweden; SERI, SNSF and Cantons of Bern and Geneva, Switzerland; NSTC, Taipei; TENMAK, Türkiye; STFC/UKRI, United Kingdom; DOE and NSF, United States of America.

Individual groups and members have received support from BCKDF, CANARIE, CRC and DRAC, Canada; CERN-CZ, FORTE and PRIMUS, Czech Republic; COST, ERC, ERDF, Horizon 2020, ICSC-NextGenerationEU and Marie Skłodowska-Curie Actions, European Union; Investissements d'Avenir Labex, Investissements d'Avenir Idex and ANR, France; DFG and AvH Foundation, Germany; Herakleitos, Thales and Aristeia programmes co-financed by EU-ESF and the Greek NSRF, Greece; BSF-NSF and MINERVA, Israel; NCN and NAWA, Poland; La Caixa Banking Foundation, CERCA and AGAUR programs from Generalitat de Catalunya and PROMETEO and GenT Programmes Generalitat Valenciana, Spain; Göran Gustafssons Stiftelse, Sweden; The Royal Society and Leverhulme Trust, United Kingdom; Eric and Wendy Schmidt Fund for Strategic Innovation, United States of America.

In addition, individual members wish to acknowledge support from Armenia: Yerevan Physics Institute (FAPERJ); CERN: European Organization for Nuclear Research (CERN DOCT); Chile: Agencia Nacional de Investigación y Desarrollo (ANID FONDECYT reg. 1230987, FONDECYT 1230812, FONDECYT 1240864, Fondecyt 3240661, Fondecyt Regular 1240721); China: Chinese Ministry of Science and Technology (MOST-2023YFA1605700, MOST-2023YFA1609300), National Natural Science Foundation of China (NSFC - 12175119, NSFC 12275265, NSFC-12075060); Czech Republic: Czech Science Foundation (GACR - 24-11373S), Ministry of Education Youth and Sports (ERC-CZ-LL2327, FORTE CZ.02.01.01/00/22_008/0004632), PRIMUS Research Programme (PRIMUS/21/SCI/017); EU: H2020 European Research Council (ERC - 101002463); European Union: European Research Council (BARD No. 101116429, ERC - 948254, ERC 101089007), Horizon 2020 Framework Programme (MUCCA - CHIST-ERA-19-XAI-00), European Union, Future Artificial Intelligence Research (FAIR-NextGenerationEU PE00000013), Italian Center for High Performance Computing, Big Data and Quantum Computing (ICSC,

NextGenerationEU), Marie Sklodowska-Curie Actions (ERC Horizon-2020, GA 956086, GAP-101168829); France: Agence Nationale de la Recherche (ANR-20-CE31-0013, ANR-21-CE31-0013, ANR-21-CE31-0022, ANR-22-EDIR-0002, ANR-24-CE31-0504-01); Germany: Baden-Württemberg Stiftung (BW Stiftung-Postdoc Eliteprogramme), Deutsche Forschungsgemeinschaft (DFG - 469666862, DFG - CR 312/5-2); Italy: Istituto Nazionale di Fisica Nucleare (ICSC, NextGenerationEU), Ministero dell'Università e della Ricerca (NextGenEU 153D23001490006 M4C2.1.1, NextGenEU I53D23000820006 M4C2.1.1, NextGenEU I53D23001490006 M4C2.1.1); Japan: Japan Society for the Promotion of Science (JSPS KAKENHI JP22H01227, JSPS KAKENHI JP22H04944, JSPS KAKENHI JP22KK0227, JSPS KAKENHI JP24K23939); Norway: Research Council of Norway (RCN-314472); Poland: Ministry of Science and Higher Education (IDUB AGH, POB8, D4 no 9722), Polish National Science Centre (NCN 2021/42/E/ST2/00350, NCN OPUS 2023/51/B/ST2/02507, NCN OPUS nr 2022/47/B/ST2/03059, NCN UMO-2019/34/E/ST2/00393, UMO-2020/37/B/ST2/01043, UMO-2022/47/O/ST2/00148, UMO-2023/49/B/ST2/04085, UMO-2023/51/B/ST2/00920); Portugal: Foundation for Science and Technology (FCT); Spain: Generalitat Valenciana (Artemisa, FEDER, IDIFEDER/2018/048, ASFAE/2022/008), Ministry of Science and Innovation (MCIN & NextGenEU PCI2022-135018-2, MICIN & FEDER PID2021-125273NB, RYC2019-028510-I, RYC2020-030254-I, RYC2021-031273-I, RYC2022-038164-I), Ministerio de Ciencia, Innovación y Universidades/Agencia Estatal de Investigación (EU NextGenerationEU (PRTR-C17.I1), PID2022-142604OB-C22); Sweden: Carl Trygger Foundation (Carl Trygger Foundation CTS 22:2312), Swedish Research Council (Swedish Research Council 2023-04654, VR 2018-00482, VR 2021-03651, VR 2022-03845, VR 2022-04683, VR 2023-03403), Knut and Alice Wallenberg Foundation (KAW 2018.0458, KAW 2019.0447, KAW 2022.0358); Switzerland: Swiss National Science Foundation (SNSF - PCEFP2_194658); United Kingdom: Leverhulme Trust (Leverhulme Trust RPG-2020-004), Royal Society (NIF-R1-231091); United States of America: U.S. Department of Energy (ECA DE-AC02-76SF00515), Neubauer Family Foundation.

The ATLAS Collaboration

G. Aad[153], E. Aakvaag[18], B. Abbott[173], S. Abdelhameed[131], K. Abeling[81], N.J. Abicht[75], S.H. Abidi[43], M. Aboelela[70], A. Aboulhorma[59], H. Abramowicz[222], Y. Abulaiti[170], B.S. Acharya[XVI,99,100], A. Ackermann[90], C. Adam Bourdarios[5], L. Adamczyk[135], S.V. Addepalli[212], M. J. Addison[152], J. Adelman[169], A. Adiguzel[26], T. Adye[193], A.A. Affolder[195], Y. Afik[64], M.N. Agaras[14], A. Aggarwal[151], C. Agheorghiesei[36], F. Ahmadov[XXXII,63], S. Ahuja[146], X. Ai[205], G. Aielli[114,115], A. Aikot[235], M. Ait Tamlihat[59], B. Aitbenchikh[55], M. Akbiyik[151], T.P.A. Åkesson[149], A.V. Akimov[214], D. Akiyama[240], N.N. Akolkar[31], S. Aktas[24], G.L. Alberghi[30], J. Albert[237], P. Albicocco[79], G.L. Albouy[87], S. Alderweireldt[78], Z.L. Alegria[174], M. Aleksa[61], I.N. Aleksandrov[63], C. Alexa[35], T. Alexopoulos[11], F. Alfonsi[30], M. Algren[82], M. Alhroob[239], B. Ali[191], H. M. J. Ali[XXV,142], S. Ali[45], S.W. Alibocus[143], M. Aliev[49], G. Alimonti[104], W. Alkakhi[81], C. Allaire[96], B.M.M. Allbrooke[215], J. S. Allen[152], J.F. Allen[78], P.P. Allport[23], A. Aloisio[106,107], F. Alonso[141], C. Alpigiani[203], Z.M.K. Alsolami[142], A. Alvarez Fernandez[151], M. Alves Cardoso[82], M.G. Alviggi[106,107], M. Aly[152], Y. Amaral Coutinho[125], A. Ambler[155], C. Amelung[61], M. Amerl[152], C.G. Ames[160], D. Amidei[157], B. Amini[80], K. Amirie[226], A. Amirkhanov[63], S.P. Amor Dos Santos[183], K.R. Amos[235], D. Amperiadou[223], S. An[129], V. Ananiev[178], C. Anastopoulos[208], T. Andeen[12], J.K. Anders[143], A. C. Anderson[86], A. Andreazza[104,105], S. Angelidakis[10], A. Angerami[66], A.V. Anisenkov[63], A. Annovi[110], C. Antel[82], E. Antipov[214], M. Antonelli[79], F. Anulli[112], M. Aoki[129], T. Aoki[224], M.A. Aparo[215], L. Aperio Bella[74], C. Appelt[222], A. Apyan[33], S. J. Arbiol Val[137], C. Arcangeletti[79], A.T.H. Arce[77], J-F. Arguin[159], S. Argyropoulos[223], J.-H. Arling[74], O. Arnaez[5], H. Arnold[214], G. Artoni[112,113], H. Asada[162], K. Asai[171], S. Asai[224], N.A. Asbah[61], R. A. Ashby Pickering[239], A. M. Aslam[146], K. Assamagan[43], R. Astalos[41], K. S. V. Astrand[149], S. Atashi[231], R.J. Atkin[47], H. Atmani[60], P.A. Atmasiddha[181], K. Augsten[191], A.D. Auriol[65], V.A. Austrup[152], G. Avolio[61], K. Axiotis[82], G. Azuelos[XXXVII,159], D. Babal[42], H. Bachacou[194], K. Bachas[XX,223], A. Bachiu[54], E. Bachmann[76], M. J. Backes[90], A. Badea[64], T.M. Baer[157], P. Bagnaia[112,113], M. Bahmani[21], D. Bahner[80], K. Bai[176], J.T. Baines[193], L. Baines[145], O.K. Baker[244], E. Bakos[17], D. Bakshi Gupta[9], L.E. Balabram Filho[125], V. Balakrishnan[173], R. Balasubramanian[5], E.M. Baldin[62], P. Balek[135], E. Ballabene[30,29], F. Balli[194], L.M. Baltes[90], W.K. Balunas[46], J. Balz[151], I. Bamwidhi[132], E. Banas[137], M. Bandieramonte[182], A. Bandyopadhyay[31], S. Bansal[31], L. Barak[222], M. Barakat[74], E.L. Barberio[156], D. Barberis[20], M. Barbero[153], M. Z. Barel[168], T. Barillari[161], M-S. Barisits[61], T. Barklow[212], P. Baron[175], D.A. Baron Moreno[152], A. Baroncelli[89], A.J. Barr[179], J.D. Barr[147], F. Barreiro[150], J. Barreiro Guimarães da Costa[15], M.G. Barros Teixeira[183], S. Barsov[62], F. Bartels[90], R. Bartoldus[212], A.E. Barton[142], P. Bartos[41], A. Basan[151], M. Baselga[75], S. Bashiri[137], A. Bassalat[II,96], M.J. Basso[227], S. Bataju[70], R. Bate[236], R.L. Bates[86], S. Batlamous[150], M. Battaglia[195], D. Battulga[21], M. Bauce[112,113], M. Bauer[120], P. Bauer[31], L. T. Bayer[74], L.T. Bazzano Hurrell[44], J.B. Beacham[161], T. Beau[180], J.Y. Beaucamp[141], P.H. Beauchemin[230], P. Bechtle[31], H.P. Beck[XIX,22], K. Becker[239], A.J. Beddall[123], V.A. Bednyakov[63], C.P. Bee[214], L.J. Beemster[17], M. Begalli[127], M. Begel[43], J.K. Behr[74], J.F. Beirer[61], F. Beisiegel[31], M. Belfkir[132], G. Bella[222], L. Bellagamba[30], A. Bellerive[54], C.D. Bellgraph[98], P. Bellos[23], K. Beloborodov[62], D. Benchekroun[55], F. Bendebba[55], Y. Benhammou[222], K.C. Benkendorfer[88], L. Beresford[74], M. Beretta[79], E. Bergeaas Kuutmann[233], N. Berger[5], B. Bergmann[191], J. Beringer[19], G. Bernardi[6], C. Bernius[212], F.U. Bernlochner[31], F. Bernon[61], A. Berrocal Guardia[14], T. Berry[146], P. Berta[192], A. Berthold[76], R. Bertrand[153], S. Bethke[161], A. Betti[112,113], A.J. Bevan[145], L. Bezio[82], N.K. Bhalla[80], S. Bharthuar[161], S. Bhatta[214], P. Bhattarai[212], Z.M. Bhatti[170], K. D. Bhide[80], V.S. Bhopatkar[174], R.M. Bianchi[182], G. Bianco[30,29], O. Biebel[160], M. Biglietti[116], C. S. Billingsley[70], Y. Bimgdi[60], M. Bindi[81], A. Bingham[243], A. Bingul[25], C. Bini[112,113], G.A. Bird[46], M. Birman[241], M. Biros[192], S. Biryukov[215], T. Bisanz[75], E. Bisceglie[30,29], J.P. Biswal[193], D. Biswas[210], I. Bloch[74], A. Blue[86], U. Blumenschein[145], J. Blumenthal[151], V.S. Bobrovnikov[63], M. Boehler[80], B. Boehm[238], D. Bogavac[61], A.G. Bogdanchikov[62], L. S. Boggia[180], V. Boisvert[146], P. Bokan[61], T. Bold[135], M. Bomben[6], M. Bona[145], M. Boonekamp[194], A.G. Borbély[86], I.S. Bordulev[62], G. Borissov[142], D. Bortoletto[179], D. Boscherini[30], M. Bosman[14], K. Bouaouda[55], N. Bouchhar[235], L. Boudet[5], J. Boudreau[182], E.V. Bouhova-Thacker[142], D. Boumediene[65], R. Bouquet[84,83], A. Boveia[172], J. Boyd[61], D. Boye[43], I.R. Boyko[63], L. Bozianu[82], J. Bracinik[23], N. Brahimi[5], G. Brandt[243], O. Brandt[46], B. Brau[154], J.E. Brau[176], R. Brener[241], L. Brenner[168], R. Brenner[233], S. Bressler[241], G. Brianti[118,119], D. Britton[86], D. Britzger[161], I. Brock[31], R. Brock[158], G. Brooijmans[66], A.J. Brooks[98], E. M. Brooks[228], E. Brost[43], L.M. Brown[237,227], L.E. Bruce[88], T.L. Bruckler[179], P.A. Bruckman de Renstrom[137], B. Brüers[74], A. Bruni[30], G. Bruni[30], D. Brunner[72,73], M. Bruschi[30], N. Bruscino[112,113], T. Buanes[18], Q. Buat[203], D. Buchin[161], A.G. Buckley[86], O. Bulekov[123], B.A. Bullard[212], S. Burdin[143], C.D. Burgard[75], A.M. Burger[61], B. Burghgrave[9], O. Burlayenko[80], J. Burleson[234], J.T.P. Burr[46], J.C. Burzynski[211], E.L. Busch[66], V. Büscher[151], P.J. Bussey[86], J.M. Butler[32], C.M. Buttar[86], J.M. Butterworth[147], W. Buttinger[193], C.J. Buxo Vazquez[158], A.R. Buzykaev[63], S. Cabrera Urbán[235], L. Cadamuro[96], D. Caforio[85], H. Cai[182], Y. Cai[30,165,29], Y. Cai[163], V.M.M. Cairo[61], O. Cakir[3], N. Calace[61], P. Calafiura[19], G. Calderini[180], P. Calfayan[54], G. Callea[86], L.P. Caloba[125], D. Calvet[65], S. Calvet[65],

R. Camacho Toro[180], S. Camarda[61], D. Camarero Munoz[33], P. Camarri[114,115], M.T. Camerlingo[106,107], C. Camincher[237], M. Campanelli[147], A. Camplani[67], V. Canale[106,107], A.C. Canbay[3], E. Canonero[146], J. Cantero[235], Y. Cao[234], F. Capocasa[33], M. Capua[69,68], A. Carbone[104,105], R. Cardarelli[114], J.C.J. Cardenas[9], M. P. Cardiff[33], G. Carducci[69,68], T. Carli[61], G. Carlino[106], J.I. Carlotto[14], B.T. Carlson[XXI,182], E.M. Carlson[237], J. Carmignani[143], L. Carminati[104,105], A. Carnelli[5], M. Carnesale[61], S. Caron[167], E. Carquin[201], I.B. Carr[156], S. Carrá[104], G. Carratta[30,29], A.M. Carroll[176], M.P. Casado[X,14], M. Caspar[74], F.L. Castillo[5], L. Castillo Garcia[14], V. Castillo Gimenez[235], N.F. Castro[183,187], A. Catinaccio[61], J.R. Catmore[178], T. Cavaliere[5], V. Cavaliere[43], L.J. Caviedes Betancourt[28], Y.C. Cekmecelioglu[74], E. Celebi[123], S. Cella[61], V. Cepaitis[82], K. Cerny[175], A.S. Cerqueira[124], A. Cerri[XLI,110], L. Cerrito[114,115], F. Cerutti[19], B. Cervato[104,105], A. Cervelli[30], G. Cesarini[79], S.A. Cetin[123], P.M. Chabrillat[180], J. Chan[19], W.Y. Chan[224], J.D. Chapman[46], E. Chapon[194], B. Chargeishvili[219], D.G. Charlton[23], C. Chauhan[192], Y. Che[163], S. Chekanov[7], S.V. Chekulaev[227], G.A. Chelkov[I,63], B. Chen[222], B. Chen[237], H. Chen[163], H. Chen[43], J. Chen[206], J. Chen[211], M. Chen[179], S. Chen[138], S.J. Chen[163], X. Chen[206], X. Chen[XXXVI,16], Z. Chen[89], C.L. Cheng[242], H.C. Cheng[92], S. Cheong[212], A. Cheplakov[63], E. Cheremushkina[74], E. Cherepanova[168], R. Cherkaoui El Moursli[59], E. Cheu[8], K. Cheung[95], L. Chevalier[194], V. Chiarella[79], G. Chiarelli[110], N. Chiedde[153], G. Chiodini[102], A.S. Chisholm[23], A. Chitan[35], M. Chitishvili[235], M.V. Chizhov[XXII,63], K. Choi[12], Y. Chou[203], E.Y.S. Chow[167], K.L. Chu[241], M.C. Chu[92], X. Chu[15,165], Z. Chubinidze[79], J. Chudoba[190], J.J. Chwastowski[137], D. Cieri[161], K.M. Ciesla[135], V. Cindro[144], A. Ciocio[19], F. Cirotto[106,107], Z.H. Citron[241], M. Citterio[104], D.A. Ciubotaru[35], A. Clark[82], P.J. Clark[78], N. Clarke Hall[147], C. Clarry[226], S.E. Clawson[74], C. Clement[72,73], Y. Coadou[153], M. Cobal[99,101], A. Coccaro[84], R.F. Coelho Barrue[183], R. Coelho Lopes De Sa[154], S. Coelli[104], L. S. Colangeli[226], B. Cole[66], P. Collado Soto[150], J. Collot[87], P. Conde Muiño[183,189], M.P. Connell[49], S.H. Connell[49], E.I. Conroy[179], M. Contreras Cossio[12], F. Conventi[XXXVIII,106], H.G. Cooke[23], A.M. Cooper-Sarkar[179], L. Corazzina[112,113], F. A. Corchia[30,29], A. Cordeiro Oudot Choi[203], L.D. Corpe[65], M. Corradi[112,113], F. Corriveau[XXX,155], A. Cortes-Gonzalez[21], M.J. Costa[235], F. Costanza[5], D. Costanzo[208], B.M. Cote[172], J. Couthures[5], G. Cowan[146], K. Cranmer[242], L. Cremer[75], D. Cremonini[30,29], S. Crépé-Renaudin[87], F. Crescioli[180], T. Cresta[108,109], M. Cristinziani[210], M. Cristoforetti[118,119], V. Croft[168], J.E. Crosby[174], G. Crosetti[69,68], A. Cueto[150], H. Cui[147], Z. Cui[8], W.R. Cunningham[86], F. Curcio[235], J. R. Curran[78], P. Czodrowski[61], M.J. Da Cunha Sargedas De Sousa[84,83], J.V. Da Fonseca Pinto[125], C. Da Via[152], W. Dabrowski[135], T. Dado[61], S. Dahbi[217], T. Dai[157], D. Dal Santo[22], C. Dallapiccola[154], M. Dam[67], G. D'amen[43], V. D'Amico[160], J. Damp[151], J.R. Dandoy[54], D. Dannheim[61], G. D'anniballe[110,111], M. Danninger[211], V. Dao[214], G. Darbo[84], S.J. Das[43], F. Dattola[74], S. D'Auria[104,105], A. D'Avanzo[106,107], T. Davidek[192], J. Davidson[239], I. Dawson[145], H.A. Day-hall[191], K. De[9], C. De Almeida Rossi[226], R. De Asmundis[106], N. De Biase[74], S. De Castro[30,29], N. De Groot[167], P. de Jong[168], H. De la Torre[169], A. De Maria[163], A. De Salvo[112], U. De Sanctis[114,115], F. De Santis[102,103], A. De Santo[215], J.B. De Vivie De Regie[87], J. Debevc[144], D.V. Dedovich[63], J. Degens[143], A.M. Deiana[70], J. Del Peso[150], L. Delagrange[180], F. Deliot[194], C.M. Delitzsch[75], M. Della Pietra[106,107], D. Della Volpe[82], A. Dell'Acqua[61], L. Dell'Asta[104,105], M. Delmastro[5], C.C. Delogu[151], P.A. Delsart[87], S. Demers[244], M. Demichev[63], S.P. Denisov[62], H. Denizli[XIV,24], L. D'Eramo[65], D. Derendarz[137], F. Derue[180], P. Dervan[XLV,143], K. Desch[31], F.A. Di Bello[84,83], A. Di Ciaccio[114,115], L. Di Ciaccio[5], A. Di Domenico[112,113], C. Di Donato[106,107], A. Di Girolamo[61], G. Di Gregorio[61], A. Di Luca[118,119], B. Di Micco[116,117], R. Di Nardo[116,117], K.F. Di Petrillo[64], M. Diamantopoulou[54], F.A. Dias[168], M.A. Diaz[196,197], A. R. Didenko[63], M. Didenko[235], E.B. Diehl[157], S. Díez Cornell[74], C. Diez Pardos[210], C. Dimitriadi[213], A. Dimitrievska[23], A. Dimri[214], J. Dingfelder[31], T. Dingley[179], I-M. Dinu[35], S.J. Dittmeier[91], F. Dittus[61], M. Divisek[192], B. Dixit[143], F. Djama[153], T. Djobava[219], C. Doglioni[152,149], A. Dohnalova[41], Z. Dolezal[192], K. Domijan[135], K.M. Dona[64], M. Donadelli[127], B. Dong[158], J. Donini[65], A. D'Onofrio[106,107], M. D'Onofrio[143], J. Dopke[193], A. Doria[106], N. Dos Santos Fernandes[183], P. Dougan[152], M.T. Dova[141], A.T. Doyle[86], M.A. Draguet[179], M.P. Drescher[81], E. Dreyer[241], I. Drivas-koulouris[11], M. Drnevich[170], M. Drozdova[82], D. Du[89], T.A. du Pree[168], F. Dubinin[63], M. Dubovsky[41], E. Duchovni[241], G. Duckeck[160], P. K. Duckett[147], O.A. Ducu[35], D. Duda[78], A. Dudarev[61], E. R. Duden[33], M. D'uffizi[152], L. Duflot[96], M. Dührssen[61], I. Duminica[40], A.E. Dumitriu[35], M. Dunford[90], S. Dungs[75], K. Dunne[72,73], A. Duperrin[153], H. Duran Yildiz[3], M. Düren[85], A. Durglishvili[219], D. Duvnjak[54], B.L. Dwyer[169], G.I. Dyckes[19], M. Dyndal[135], B.S. Dziedzic[61], Z.O. Earnshaw[215], G.H. Eberwein[179], B. Eckerova[41], S. Eggebrecht[81], E. Egidio Purcino De Souza[128], G. Eigen[18], K. Einsweiler[19], T. Ekelof[233], P.A. Ekman[149], S. El Farkh[56], Y. El Ghazali[89], H. El Jarrari[61], A. El Moussaouy[55], V. Ellajosyula[233], M. Ellert[233], F. Ellinghaus[243], N. Ellis[61], J. Elmsheuser[43], M. Elsawy[131], M. Elsing[61], D. Emeliyanov[193], Y. Enari[129], I. Ene[19], S. Epari[159], D. Ernani Martins Neto[137], F. Ernst[61], M. Errenst[243], M. Escalier[96], C. Escobar[235], E. Etzion[222], G. Evans[183,184], H. Evans[98], L.S. Evans[146], A. Ezhilov[62], S. Ezzarqtouni[55], F. Fabbri[30,29], L. Fabbri[30,29], G. Facini[147], V. Fadeyev[195], R.M. Fakhrutdinov[62], D. Fakoudis[151], S. Falciano[112], L.F. Falda Ulhoa Coelho[183], F. Fallavollita[161], G. Falsetti[69,68], J. Faltova[192], C. Fan[234], K. Y. Fan[93], Y. Fan[15], Y. Fang[15,165], M. Fanti[104,105], M. Faraj[99,100], Z. Farazpay[148], A. Farbin[9], A. Farilla[116], T. Farooque[158], J. N. Farr[244], S.M. Farrington[193,78], F. Fassi[59], D. Fassouliotis[10], L. Fayard[96], P. Federic[192], P. Federicova[190], O.L. Fedin[I,62], M. Feickert[242], L. Feligioni[153], D.E. Fellers[19], C. Feng[204], Z. Feng[168], M.J. Fenton[231], L. Ferencz[74], B. Fernandez Barbadillo[142], P. Fernandez Martinez[97], M.J.V. Fernoux[153], J. Ferrando[142], A. Ferrari[233], P. Ferrari[168,167], R. Ferrari[108], D. Ferrere[82], C. Ferretti[157], M. P. Fewell[1], D. Fiacco[112,113], F. Fiedler[151], P. Fiedler[191], S. Filimonov[63], A. Filipčič[144], E.K. Filmer[227], F. Filthaut[167], M.C.N. Fiolhais[III,183,185], L. Fiorini[235], W.C. Fisher[158], T. Fitschen[152], P. M. Fitzhugh[194], I. Fleck[210], P. Fleischmann[157], T. Flick[243], M. Flores[XXXIV,50], L.R. Flores Castillo[92], L. Flores Sanz De Acedo[61], F.M. Follega[118,119], N. Fomin[46], J.H. Foo[226], A. Formica[194], A.C. Forti[152], E. Fortin[61], A.W. Fortman[19], L. Foster[19], L. Fountas[XI,10], D. Fournier[96], H. Fox[142], P. Francavilla[110,111], S. Francescato[88], S. Franchellucci[82], M. Franchini[30,29], S. Franchino[90], D. Francis[61], L. Franco[167], V. Franco Lima[61], L. Franconi[74], M. Franklin[88], G. Frattari[33], Y.Y. Frid[222], J. Friend[86], N. Fritzsche[61], A. Froch[82], D. Froidevaux[61], J.A. Frost[179], Y. Fu[158], S. Fuenzalida Garrido[201], M. Fujimoto[153], K. Y. Fung[92], E. Furtado De Simas Filho[128], M. Furukawa[224], J. Fuster[235], A. Gaa[81], A. Gabrielli[30,29], A. Gabrielli[226], P. Gadow[61], G. Gagliardi[84,83], L.G. Gagnon[19], S. Gaid[133], S. Galantzan[222], J. Gallagher[1], E.J. Gallas[179], A.L. Gallen[233], B.J. Gallop[193], K.K. Gan[172], S. Ganguly[224], Y. Gao[78], A. Garabaglu[203], F.M. Garay Walls[196,197], C. García[235], A. Garcia Alonso[168], A.G. Garcia Caffaro[244], J.E. García Navarro[235], M. Garcia-Sciveres[19], G.L. Gardner[181], R.W. Gardner[64], N. Garelli[230], R.B. Garg[212], J.M. Gargan[78], C.A. Garner[226], C.M. Garvey[47], V. K. Gassmann[230], G. Gaudio[108], V. Gautam[14], P. Gauzzi[112,113], J. Gavranovic[144], I.L. Gavrilenko[183], A. Gavrilyuk[62], C. Gay[236], G. Gaycken[176], E.N. Gazis[11], A. Gekow[172], C. Gemme[84], M.H. Genest[87], A. D. Gentry[166], S. George[146], W.F. George[23], T. Geralis[71], A. A. Gerwin[173], P. Gessinger-Befurt[61], M.E. Geyik[243], M. Ghani[239], K. Ghorbanian[145], A. Ghosal[210], A. Ghosh[231], A. Ghosh[8], B. Giacobbe[30], S. Giagu[112,113], T. Giani[168], A. Giannini[89], S.M. Gibson[146], M. Gignac[195], D.T.

Gil[136], A.K. Gilbert[135], B.J. Gilbert[66], D. Gillberg[54], G. Gilles[168], D.M. Gingrich[XXXVII,2], M.P. Giordani[99,101], P.F. Giraud[194], G. Giugliarelli[99,101], D. Giugni[104], F. Giuli[114,115], I. Gkialas[XI,10], L.K. Gladilin[62], C. Glasman[150], G. Glemža[74], M. Glisic[176], I. Gnesi[69], Y. Go[43], M. Goblirsch-Kolb[61], B. Gocke[75], D. Godin[159], B. Gokturk[24], S. Goldfarb[156], T. Golling[82], M.G.D. Gololo[49], D. Golubkov[62], J.P. Gombas[158], A. Gomes[183,184], G. Gomes Da Silva[210], A.J. Gomez Delegido[235], R. Gonçalo[183], L. Gonella[23], A. Gongadze[220], F. Gonnella[23], J.L. Gonski[212], R.Y. González Andana[78], S. González de la Hoz[235], C. Gonzalez Renteria[19], M. V. Gonzalez Rodrigues[74], R. Gonzalez Suarez[233], S. Gonzalez-Sevilla[82], L. Goossens[61], B. Gorini[61], E. Gorini[102,103], A. Gorišek[144], T.C. Gosart[181], A.T. Goshaw[77], M.I. Gostkin[63], S. Goswami[174], C.A. Gottardo[61], S. A. Gotz[160], M. Gouighri[56], A.G. Goussiou[203], N. Govender[49], R. P. Grabarczyk[179], I. Grabowska-Bold[135], K. Graham[54], E. Gramstad[178], S. Grancagnolo[102,103], C.M. Grant[1,194], P.M. Gravila[39], F.G. Gravili[102,103], H.M. Gray[19], M. Greco[161], M. J. Green[1], C. Grefe[31], A. S. Grefsrud[18], I.M. Gregor[74], K.T. Greif[231], P. Grenier[212], S.G. Grewe[161], A.A. Grillo[195], K. Grimm[45], S. Grinstein[XXVI,14], J.-F. Grivaz[96], E. Gross[241], J. Grosse-Knetter[81], L. Guan[157], G. Guerrieri[61], R. Guevara[178], R. Gugel[151], J.A.M. Guhit[157], A. Guida[21], E. Guilloton[239], S. Guindon[61], F. Guo[15,165], J. Guo[206], L. Guo[74], L. Guo[XXIV,164], Y. Guo[157], A. Gupta[75], R. Gupta[182], S. Gupta[33], S. Gurbuz[31], S.S. Gurdasani[74], G. Gustavino[112,113], P. Gutierrez[173], L.F. Gutierrez Zagazeta[181], M. Gutsche[76], C. Gutschow[147], C. Gwenlan[179], C.B. Gwilliam[143], E.S. Haaland[178], A. Haas[170], M. Habedank[86], C. Haber[19], H.K. Hadavand[9], A. Haddad[65], A. Hadef[76], A.I. Hagan[142], J. J. Hahn[210], E.H. Haines[147], M. Haleem[238], J. Haley[174], G.D. Hallewell[153], L. Halser[22], K. Hamano[237], M. Hamer[31], S. E. D. Hammoud[96], E.J. Hampshire[146], J. Han[204], L. Han[163], L. Han[89], S. Han[19], K. Hanagaki[129], M. Hance[195], D.A. Hangal[66], H. Hanif[211], M.D. Hank[181], J.B. Hansen[67], P.H. Hansen[67], D. Harada[82], T. Harenberg[243], S. Harkusha[245], M.L. Harris[154], Y.T. Harris[31], J. Harrison[14], N.M. Harrison[172], P.F. Harrison[239], M. L. E. Hart[147], N.M. Hartman[161], N.M. Hartmann[160], R. Z. Hasan[146,193], Y. Hasegawa[209], F. Haslbeck[179], S. Hassan[18], R. Hauser[158], M. Haviernik[192], C.M. Hawkes[23], R.J. Hawkings[61], Y. Hayashi[224], D. Hayden[158], C. Hayes[157], R.L. Hayes[168], C.P. Hays[179], J.M. Hays[145], H.S. Hayward[143], F. He[89], M. He[15,165], Y. He[74], Y. He[147], N.B. Heatley[145], V. Hedberg[149], A.L. Heggelund[178], C. Heidegger[80], K.K. Heidegger[80], J. Heilman[54], S. Heim[74], T. Heim[19], J.G. Heinlein[181], J.J. Heinrich[176], L. Heinrich[XXXV,161], J. Hejbal[190], A. Held[242], S. Hellesund[18], C.M. Helling[236], S. Hellman[72,73], L. Henkelmann[46], A.M. Henriques Correia[61], H. Herde[149], Y. Hernández Jiménez[214], L.M. Herrmann[31], T. Herrmann[76], G. Herten[80], R. Hertenberger[160], L. Hervas[61], M.E. Hesping[151], N.P. Hessey[227], J. Hessler[161], M. Hidaoui[56], N. Hidic[192], E. Hill[226], S.J. Hillier[23], J.R. Hinds[158], F. Hinterkeuser[31], M. Hirose[177], S. Hirose[229], D. Hirschbuehl[243], T.G. Hitchings[152], B. Hiti[144], J. Hobbs[214], R. Hobincu[38], N. Hod[241], M.C. Hodgkinson[208], B.H. Hodkinson[179], A. Hoecker[61], D. D. Hofer[157], J. Hofer[235], M. Holzbock[61], L.B.A.H. Hommels[46], V. Homsak[179], B.P. Honan[152], J. J. Hong[98], J. Hong[206], T.M. Hong[182], B.H. Hooberman[234], W.H. Hopkins[7], M. C. Hoppesch[234], Y. Horii[162], M. E. Horstmann[161], S. Hou[217], M. R. Housenga[234], A.S. Howard[144], J. Howarth[86], J. Hoya[7], M. Hrabovsky[175], T. Hryn'ova[5], P.J. Hsu[95], S.-C. Hsu[203], T. Hsu[96], M. Hu[19], Q. Hu[89], S. Huang[46], X. Huang[15,165], Y. Huang[192], Y. Huang[164], Y. Huang[151], Y. Huang[15], Z. Huang[96], Z. Hubacek[191], M. Huebner[31], F. Huegging[31], T.B. Huffman[179], M. Hufnagel Maranha De Faria[124], C. A. Hugli[74], M. Huhtinen[61], S.K. Huiberts[18], R. Hulsken[155], C. E. Hultquist[19], N. Huseynov[VIII,13], J. Huston[158], J. Huth[88], R. Hyneman[8], G. Iacobucci[82], G. Iakovidis[43], L. Iconomidou-Fayard[96], J. P. Iddon[61], P. Iengo[106,107], R. Iguchi[224], Y. Iiyama[224], T. Iizawa[179], Y. Ikegami[129], D. Iliadis[223], N. Ilic[226], H. Imam[126], G. Inacio Goncalves[127], S. A. Infante Cabanas[198], T. Ingebretsen Carlson[72,73], J. M. Inglis[145], G. Introzzi[108,109], M. Iodice[116], V. Ippolito[112,113], R. K. Irwin[143], M. Ishino[224], W. Islam[242], C. Issever[21], S. Istin[XLIV,24], K. Itabashi[129], H. Ito[240], R. Iuppa[118,119], A. Ivina[241], V. Izzo[106], P. Jacka[190], P. Jackson[1], P. Jain[74], K. Jakobs[80], T. Jakoubek[241], J. Jamieson[86], W. Jang[224], S. Jankovych[192], M. Javurkova[154], P. Jawahar[152], L. Jeanty[176], J. Jejelava[XXXIII,218], P. Jenni[VII,80], C.E. Jessiman[54], C. Jia[204], H. Jia[236], J. Jia[214], X. Jia[15,165], Z. Jia[163], C. Jiang[78], Q. Jiang[93], S. Jiggins[74], M. Jimenez Ortega[235], J. Jimenez Pena[14], S. Jin[163], A. Jinaru[35], O. Jinnouchi[202], P. Johansson[208], K.A. Johns[8], J.W. Johnson[195], F. A. Jolly[74], D.M. Jones[215], E. Jones[74], K.S. Jones[9], P. Jones[46], R.W.L. Jones[142], T.J. Jones[143], H.L. Joos[81,61], R. Joshi[172], J. Jovicevic[17], X. Ju[19], J.J. Junggeburth[61], T. Junkermann[90], A. Juste Rozas[XXVI,14], M.K. Juzek[137], S. Kabana[200], A. Kaczmarska[137], M. Kado[161], H. Kagan[172], M. Kagan[212], A. Kahn[181], C. Kahra[151], T. Kaji[224], E. Kajomovitz[221], N. Kakati[241], N. Kakoty[14], I. Kalaitzidou[80], S. Kandel[9], N.J. Kang[195], D. Kar[XLV,53], K. Karava[179], E. Karentzos[31], O. Karkout[168], S.N. Karpov[63], Z.M. Karpova[63], V. Kartvelishvili[142], A.N. Karyukhin[62], E. Kasimi[223], J. Katzy[74], S. Kaur[54], K. Kawade[209], M.P. Kawale[173], C. Kawamoto[138], T. Kawamoto[89], E.F. Kay[61], F.I. Kaya[230], S. Kazakos[158], V.F. Kazanin[62], Y. Ke[214], J.M. Keaveney[47], R. Keeler[237], G.V. Kehris[88], J.S. Keller[54], J.J. Kempster[215], O. Kepka[190], J. Kerr[228], B.P. Kerridge[193], B.P. Kerševan[144], L. Keszeghova[41], R. A. Khan[182], A. Khanov[174], A.G. Kharlamov[62], T. Kharlamova[62], E.E. Khoda[203], M. Kholodenko[183], T.J. Khoo[21], G. Khoriauli[238], Y. Khoulaki[55], J. Khubua[XLV,219], Y.A.R. Khwaira[180], B. Kibirige[53], D. Kim[7], D.W. Kim[72,73], Y.K. Kim[64], N. Kimura[147], M.K. Kingston[81], A. Kirchhoff[81], C. Kirfel[31], F. Kirfel[31], J. Kirk[193], A.E. Kiryunin[161], S. Kita[229], C. Kitsaki[11], O. Kivernyk[31], M. Klassen[230], C. Klein[54], L. Klein[238], M.H. Klein[70], S.B. Klein[82], U. Klein[143], A. Klimentov[43], T. Klioutchnikova[61], P. Kluit[168], S. Kluth[161], E. Kneringer[120], T.M. Knight[226], A. Knue[75], M. Kobel[76], D. Kobylianskii[241], S.F. Koch[179], M. Kocian[212], P. Kodyš[192], D.M. Koeck[176], P.T. Koenig[31], T. Koffas[54], O. Kolay[76], I. Koletsou[5], T. Komarek[137], K. Köneke[81], A.X.Y. Kong[1], T. Kono[171], N. Konstantinidis[147], P. Kontaxakis[82], B. Konya[149], R. Kopeliansky[66], S. Koperny[135], K. Korcyl[137], K. Kordas[V,223], A. Korn[147], S. Korn[81], I. Korolkov[14], N. Korotkova[62], B. Kortman[168], O. Kortner[161], S. Kortner[161], W.H. Kostecka[169], M. Kostov[41], V.V. Kostyukhin[210], A. Kotsokechagia[61], A. Kotwal[77], A. Koulouris[61], A. Kourkoumeli-Charalampidi[108,109], C. Kourkoumelis[10], E. Kourlitis[161], O. Kovanda[176], R. Kowalewski[237], W. Kozanecki[176], A.S. Kozhin[62], V.A. Kramarenko[62], G. Kramberger[144], P. Kramer[31], M.W. Krasny[180], A. Krasznahorkay[154], A. C. Kraus[169], J.W. Kraus[243], J.A. Kremer[74], N. B. Krengel[210], T. Kresse[76], L. Kretschmann[243], J. Kretzschmar[143], K. Kreul[21], P. Krieger[226], K. Krizka[23], K. Kroeninger[75], H. Kroha[161], J. Kroll[190], J. Kroll[181], K.S. Krowpman[158], U. Kruchonak[63], H. Krüger[31], N. Krumnack[122], M.C. Kruse[77], O. Kuchinskaia[63], S. Kuday[3], S. Kuehn[61], R. Kuesters[80], T. Kuhl[74], V. Kukhtin[63], Y. Kulchitsky[63], S. Kuleshov[199,197], J. Kull[1], M. Kumar[53], N. Kumari[74], P. Kumari[228], A. Kupco[190], T. Kupfer[75], A. Kupich[62], O. Kuprash[80], H. Kurashige[134], L.L. Kurchaninov[227], O. Kurdysh[5], Y.A. Kurochkin[62], A. Kurova[62], M. Kuze[202], A.K. Kvam[154], J. Kvita[175], N.G. Kyriacou[157], L.A.O. Laatu[153], C. Lacasta[235], F. Lacava[112,113], H. Lacker[21], D. Lacour[180], N.N. Lad[147], E. Ladygin[63], A. Lafarge[65], B. Laforge[180], T. Lagouri[244], F.Z. Lahbabi[55], S. Lai[81], J.E. Lambert[237], S. Lammers[98], W. Lampl[8], C. Lampoudis[V,223], G. Lamprinoudis[151], A.N. Lancaster[169], E. Lançon[43], U. Landgraf[80], M.P.J. Landon[145], V.S. Lang[80], O. K. B. Langrekken[178], A.J. Lankford[231], F. Lanni[61], K. Lantzsch[31], A. Lanza[108], M. Lanzac Berrocal[235], J.F. Laporte[194], T. Lari[104], D. Larsen[18], L. Larson[12], F. Lasagni Manghi[30], M. Lassnig[61], V. Latonova[190], S.D. Lawlor[208], Z. Lawrence[152],

R. Lazaridou[239], M. Lazzaroni[104,105], H. D. M. Le[158], E.M. Le Boulicaut[244], L.T. Le Pottier[19], B. Leban[30,29], M. LeBlanc[152], F. Ledroit-Guillon[87], S.C. Lee[217], T.F. Lee[143], L.L. Leeuw[XLII,49], M. Lefebvre[237], C. Leggett[19], G. Lehmann Miotto[61], M. Leigh[82], W.A. Leight[154], W. Leinonen[167], A. Leisos[XXIII,223], M.A.L. Leite[126], C.E. Leitgeb[21], R. Leitner[192], K.J.C. Leney[70], T. Lenz[31], S. Leone[110], C. Leonidopoulos[78], A. Leopold[213], J. LePage-Bourbonnais[54], R. Les[158], C.G. Lester[46], M. Levchenko[62], J. Levêque[5], L.J. Levinson[241], G. Levrini[30,29], M.P. Lewicki[137], C. Lewis[203], D.J. Lewis[5], L. Lewitt[208], A. Li[43], B. Li[204], C. Li[157], C-Q. Li[161], H. Li[89], H. Li[204], H. Li[152], H. Li[16], H. Li[89], H. Li[204], J. Li[206], K. Li[15], L. Li[206], R. Li[244], S. Li[15,165], S. Li[IV,207,206], T. Li[6], X. Li[155], Z. Li[224], Z. Li[15,165], Z. Li[89], S. Liang[15,165], Z. Liang[15], M. Liberatore[194], B. Liberti[114], K. Lie[94], J. Lieber Marin[128], H. Lien[98], H. Lin[157], S. F. Lin[214], L. Linden[160], R.E. Lindley[8], J.H. Lindon[2], J. Ling[88], E. Lipeles[181], A. Lipniacka[18], A. Lister[236], J.D. Little[98], B. Liu[15], B.X. Liu[164], D. Liu[207,206], E. H. L. Liu[23], J.K.K. Liu[46], K. Liu[207], K. Liu[207,206], M. Liu[89], M.Y. Liu[89], P. Liu[15], Q. Liu[207,203,206], X. Liu[89], X. Liu[204], Y. Liu[164,165], Y.L. Liu[204], Y.W. Liu[89], Z. Liu[XIII,96], S.L. Lloyd[145], E.M. Lobodzinska[74], P. Loch[8], E. Lodhi[226], T. Lohse[21], K. Lohwasser[208], E. Loiacono[74], J. D. Lomas[23], J.D. Long[66], I. Longarini[231], R. Longo[234], A. Lopez Solis[74], N.A. Lopez-canelas[8], N. Lorenzo Martinez[5], A.M. Lory[160], M. Losada[131], G. Löschcke Centeno[215], X. Lou[72,73], X. Lou[15,165], A. Lounis[96], P.A. Love[142], G. Lu[15,165], M. Lu[96], S. Lu[181], Y.J. Lu[217], H.J. Lubatti[203], C. Luci[112,113], F.L. Lucio Alves[163], F. Luehring[98], B. S. Lunday[181], O. Lundberg[213], J. Lunde[61], B. Lund-Jensen[XLV,213], N.A. Luongo[7], M.S. Lutz[61], A.B. Lux[32], D. Lynn[43], R. Lysak[190], V. Lysenko[191], E. Lytken[149], V. Lyubushkin[63], T. Lyubushkina[63], M.M. Lyukova[214], H. Ma[43], K. Ma[89], L.L. Ma[204], W. Ma[89], Y. Ma[174], J.C. MacDonald[151], P.C. Machado De Abreu Farias[128], R. Madar[65], T. Madula[147], J. Maeda[134], T. Maeno[43], P.T. Mafa[XII,49], H. Maguire[208], V. Maiboroda[96], A. Maio[183,184,186], K. Maj[135], O. Majersky[74], S. Majewski[176], R. Makhmanazarov[62], N. Makovec[96], V. Maksimovic[17], B. Malaescu[180], J. Malamant[178], Pa. Malecki[137], V.P. Maleev[62], F. Malek[XVIII,87], M. Mali[144], D. Malito[146], U. Mallik[XLV,121], A. Maloizel[6], S. Maltezos[11], A. Malvezzi Lopes[127], S. Malyukov[63], J. Mamuzic[14], G. Mancini[79], M. N. Mancini[33], G. Manco[108,109], J.P. Mandalia[145], S.S. Mandarry[215], I. Mandić[144], L. Manhaes de Andrade Filho[124], I.M. Maniatis[241], J. Manjarres Ramos[140], D.C. Mankad[241], A. Mann[160], T. Manoussos[61], M.N. Mantinan[64], S. Manzoni[61], L. Mao[206], X. Mapekula[49], A. Marantis[XXIII,223], R.R. Marcelo Gregorio[145], G. Marchiori[6], M. Marcisovsky[190], C. Marcon[104], M. Marinescu[23], S. Marium[74], M. Marjanovic[173], A. Markhoos[80], M. Markovitch[96], M. K. Maroun[154], G. T. Marsden[152], E.J. Marshall[142], Z. Marshall[19], S. Marti-Garcia[235], J. Martin[147], T.A. Martin[193], V.J. Martin[78], B. Martin dit Latour[18], L. Martinelli[112,113], M. Martinez[XXVI,14], P. Martinez Agullo[235], V.I. Martinez Outschoorn[154], P. Martinez Suarez[14], S. Martin-Haugh[193], G. Martinovicova[192], V.S. Martoiu[35], A.C. Martyniuk[147], A. Marzin[61], D. Mascione[118,119], L. Masetti[151], J. Masik[152], A.L. Maslennikov[63], S.L. Mason[66], P. Massarotti[106,107], P. Mastrandrea[110,111], A. Mastroberardino[69,68], T. Masubuchi[177], T.T. Mathew[176], J. Matousek[192], D.M. Mattern[75], J. Maurer[35], T. Maurin[86], A.J. Maury[96], B. Maček[144], C. Mavungu Tsava[153], D.A. Maximov[62], A. E. May[152], E. Mayer[65], R. Mazini[53], I. Maznas[169], M. Mazza[158], S.M. Mazza[195], E. Mazzeo[104,105], J.P. Mc Gowan[237], S.P. Mc Kee[157], C.A. Mc Lean[7], C.C. McCracken[236], E.F. McDonald[156], A.E. McDougall[168], L. F. Mcelhinney[142], J.A. Mcfayden[215], R.P. McGovern[181], R.P. Mckenzie[53], T.C. Mclachlan[74], D.J. Mclaughlin[147], S.J. McMahon[193], C.M. Mcpartland[143], R.A. McPherson[XXX,237], S. Mehlhase[160], A. Mehta[143], D. Melini[235], B.R. Mellado Garcia[53], A.H. Melo[81], F. Meloni[74], A.M. Mendes Jacques Da Costa[152], H.Y. Meng[226], L. Meng[142], S. Menke[161], M. Mentink[61], E. Meoni[69,68], G. Mercado[169], S. Merianos[223], C. Merlassino[99,101], C. Meroni[104,105], J. Metcalfe[7], A.S. Mete[7], E. Meuser[151], C. Meyer[98], J-P. Meyer[194], R.P. Middleton[193], M. Mihovilovic[96], L. Mijović[78], G. Mikenberg[241], M. Mikestikova[190], M. Mikuž[144], H. Mildner[151], A. Milic[61], D.W. Miller[64], E. H. Miller[212], L.S. Miller[54], A. Milov[241], D.A. Milstead[72,73], T. Min[163], A.A. Minaenko[62], I.A. Minashvili[219], A.I. Mincer[170], B. Mindur[135], M. Mineev[63], Y. Mino[138], L.M. Mir[14], M. Miralles Lopez[86], M. Mironova[19], M. Missio[167], A. Mitra[239], V.A. Mitsou[235], Y. Mitsumori[162], O. Miu[226], P.S. Miyagawa[145], T. Mkrtchyan[90], M. Mlinarevic[147], T. Mlinarevic[147], M. Mlynarikova[61], S. Mobius[22], P. Mogg[160], M. H. Mohamed Farook[166], A.F. Mohammed[15,165], S. Mohapatra[66], M.F. Mohd Soberi[78], S. Mohiuddin[174], G. Mokgatitswane[53], L. Moleri[241], U. Molinatti[179], L.G. Mollier[22], B. Mondal[210], S. Mondal[191], K. Mönig[74], E. Monnier[153], L. Monsonis Romero[235], J. Montejo Berlingen[14], A. Montella[72,73], M. Montella[172], F. Montereali[116,117], F. Monticelli[141], S. Monzani[99,101], A. Morancho Tarda[67], N. Morange[96], A.L. Moreira De Carvalho[74], M. Moreno Llácer[235], C. Moreno Martinez[82], J.M. Moreno Perez[28], P. Morettini[84], S. Morgenstern[61], M. Morii[88], M. Morinaga[224], M. Moritsu[139], F. Morodei[112,113], P. Moschovakos[61], B. Moser[179], M. Mosidze[219], T. Moskalets[70], P. Moskvitina[167], J. Moss[XV,45], P. Moszkowicz[135], A. Moussa[58], Y. Moyal[241], H. Moyano Gomez[14], E.J.W. Moyse[154], O. Mtintsilana[53], S. Muanza[153], J. Mueller[182], G.A. Mullier[233], A.J. Mullin[46], J.J. Mullin[77], A.E. Mulski[88], D.P. Mungo[226], D. Munoz Perez[235], F.J. Munoz Sanchez[152], M. Murin[152], W.J. Murray[239,193], M. Muškinja[144], C. Mwewa[74], A.G. Myagkov[I,62], A.J. Myers[9], G. Myers[157], M. Myska[191], B.P. Nachman[19], K. Nagai[179], K. Nagano[129], R. Nagasaka[224], J.L. Nagle[XL,43], E. Nagy[153], A.M. Nairz[61], Y. Nakahama[129], K. Nakamura[129], K. Nakkalil[6], H. Nanjo[177], E.A. Narayanan[70], Y. Narukawa[224], I. Naryshkin[62], L. Nasella[104,105], S. Nasri[132], C. Nass[31], G. Navarro[27], J. Navarro-Gonzalez[235], A. Nayaz[21], P.Y. Nechaeva[62], S. Nechaeva[30,29], F. Nechansky[190], L. Nedic[179], T.J. Neep[23], A. Negri[108,109], M. Negrini[30], C. Nellist[168], C. Nelson[155], K. Nelson[157], S. Nemecek[190], M. Nessi[IX,61], M.S. Neubauer[234], J. Newell[143], P.R. Newman[23], Y.W.Y. Ng[234], B. Ngair[131], H.D.N. Nguyen[159], J.D. Nichols[173], R.B. Nickerson[179], R. Nicolaidou[194], J. Nielsen[195], M. Niemeyer[81], J. Niermann[61], N. Nikiforou[61], V. Nikolaenko[I,62], I. Nikolic-Audit[180], P. Nilsson[43], I. Ninca[74], G. Ninio[222], A. Nisati[112], N. Nishu[2], R. Nisius[161], N. Nitika[99,101], J-E. Nitschke[76], E.K. Nkadimeng[53], T. Nobe[224], T. Nommensen[216], M.B. Norfolk[208], B.J. Norman[54], M. Noury[55], J. Novak[144], T. Novak[144], R. Novotny[166], L. Nozka[175], K. Ntekas[231], N.M.J. Nunes De Moura Junior[125], J. Ocariz[180], A. Ochi[134], I. Ochoa[183], S. Oerdek[74], J.T. Offermann[64], A. Ogrodnik[192], A. Oh[152], C.C. Ohm[213], H. Oide[129], R. Oishi[224], M.L. Ojeda[61], Y. Okumura[224], L.F. Oleiro Seabra[183], I. Oleksiyuk[82], S.A. Olivares Pino[199], G. Oliveira Correa[14], D. Oliveira Damazio[43], J.L. Oliver[231], Ö.O. Öncel[80], A.P. O'Neill[22], A. Onofre[VI,183,187], P.U.E. Onyisi[12], M.J. Oreglia[64], D. Orestano[116,117], R. Orlandini[116,117], R.S. Orr[226], L.M. Osojnak[181], Y. Osumi[162], G. Otero y Garzón[44], H. Otono[139], G.J. Ottino[19], M. Ouchrif[58], F. Ould-Saada[178], T. Ovsiannikova[203], M. Owen[86], R.E. Owen[193], V.E. Ozcan[24], F. Ozturk[137], N. Ozturk[9], S. Ozturk[123], H.A. Pacey[179], K. Pachal[227], A. Pacheco Pages[14], C. Padilla Aranda[14], G. Padovano[112,113], S. Pagan Griso[19], G. Palacino[98], A. Palazzo[102,103], J. Pampel[31], J. Pan[244], T. Pan[92], D.K. Panchal[12], C.E. Pandini[168], J.G. Panduro Vazquez[193], H.D. Pandya[1], H. Pang[194], P. Pani[74], G. Panizzo[99,101], L. Panwar[180], L. Paolozzi[82], S. Parajuli[234], A. Paramonov[7], C. Paraskevopoulos[79], D. Paredes Hernandez[93], A. Pareti[108,109], K.R. Park[66], T.H. Park[161], F. Parodi[84,83], J.A. Parsons[66], U. Parzefall[80], B. Pascual Dias[65], L. Pascual Dominguez[150], E. Pasqualucci[112], S. Passaggio[84], F. Pastore[146], P. Patel[137], U.M. Patel[77], J.R. Pater[152], T. Pauly[61], F. Pauwels[192], C.I. Pazos[230], M. Pedersen[178], R. Pedro[183], S.V. Peleganchuk[62], O. Penc[61], E.A. Pender[78], S. Peng[16], G. D. Penn[244], K.E. Penski[160], M. Penzin[62],

B.S. Peralva[127], A.P. Pereira Peixoto[203], L. Pereira Sanchez[212], D.V. Perepelitsa[XL,43], G. Perera[154], E. Perez Codina[227], M. Perganti[11], H. Pernegger[61], S. Perrella[112,113], O. Perrin[65], K. Peters[74], R.F.Y. Peters[152], B.A. Petersen[61], T.C. Petersen[67], E. Petit[153], V. Petousis[191], A. R. Petri[104,105], C. Petridou[V,223], T. Petru[192], A. Petrukhin[210], M. Pettee[19], A. Petukhov[123], K. Petukhova[61], R. Pezoa[201], L. Pezzotti[30,29], G. Pezzullo[244], L. Pfaffenbichler[61], A. J. Pfleger[61], T.M. Pham[242], T. Pham[156], P.W. Phillips[193], G. Piacquadio[214], E. Pianori[19], F. Piazza[176], R. Piegaia[44], D. Pietreanu[35], A.D. Pilkington[152], M. Pinamonti[99,101], J.L. Pinfold[2], B.C. Pinheiro Pereira[183], J. Pinol Bel[14], A. E. Pinto Pinoargote[180], L. Pintucci[99,101], K. M. Piper[215], A. Pirtikoski[82], D.A. Pizzi[54], L. Pizzimento[93], A. Plebani[46], M.-A. Pleier[43], V. Pleskot[192], E. Plotnikova[63], G. Poddar[145], R. Poettgen[149], L. Poggioli[180], S. Polacek[192], G. Polesello[108], A. Poley[211,227], A. Polini[30], C.S. Pollard[239], Z.B. Pollock[172], E. Pompa Pacchi[173], N. I. Pond[147], D. Ponomarenko[98], L. Pontecorvo[61], S. Popa[34], G.A. Popeneciu[37], A. Poreba[61], D.M. Portillo Quintero[227], S. Pospisil[191], M. A. Postill[208], P. Postolache[36], K. Potamianos[239], P.A. Potepa[135], I.N. Potrap[63], C.J. Potter[46], H. Potti[216], J. Poveda[235], M.E. Pozo Astigarraga[61], A. Prades Ibanez[114,115], J. Pretel[237], D. Price[152], M. Primavera[102], L. Primomo[99,101], M.A. Principe Martin[150], R. Privara[175], T. Procter[86], M.L. Proffitt[203], N. Proklova[181], K. Prokofiev[94], G. Proto[161], J. Proudfoot[7], M. Przybycien[135], W.W. Przygoda[136], A. Psallidas[71], J.E. Puddefoot[208], D. Pudzha[79], D. Pyatiizbyantseva[167], J. Qian[157], R. Qian[158], D. Qichen[152], Y. Qin[14], T. Qiu[78], A. Quadt[81], M. Queitsch-Maitland[152], G. Quetant[82], R.P. Quinn[236], G. Rabanal Bolanos[88], D. Rafanoharana[80], F. Raffaeli[114,115], F. Ragusa[104,105], J.L. Rainbolt[64], J.A. Raine[82], S. Rajagopalan[43], E. Ramakoti[63], L. Rambelli[84,83], I.A. Ramirez-Berend[54], K. Ran[74,165], D. S. Rankin[181], N.P. Rapheeha[53], H. Rasheed[35], V. Raskina[180], D.F. Rassloff[90], A. Rastogi[19], S. Rave[151], S. Ravera[84,83], B. Ravina[61], I. Ravinovich[241], M. Raymond[61], A.L. Read[178], N.P. Readioff[208], D.M. Rebuzzi[108,109], A. S. Reed[161], K. Reeves[33], J.A. Reidelsturz[243], D. Reikher[176], A. Rej[75], C. Rembser[61], H. Ren[89], M. Renda[35], F. Renner[74], A.G. Rennie[86], A.L. Rescia[74], S. Resconi[104], M. Ressegotti[84], S. Rettie[61], W.F. Rettie[54], J.G. Reyes Rivera[158], E. Reynolds[19], O.L. Rezanova[63], P. Reznicek[192], H. Riani[58], N. Ribaric[77], E. Ricci[118,119], R. Richter[161], S. Richter[72,73], E. Richter-Was[136], M. Ridel[180], S. Ridouani[58], P. Rieck[170], P. Riedler[61], E.M. Riefel[72,73], J. O. Rieger[168], M. Rijssenbeek[214], M. Rimoldi[61], L. Rinaldi[30,29], P. Rincke[81], G. Ripellino[233], I. Riu[14], J.C. Rivera Vergara[237], F. Rizatdinova[174], E. Rizvi[145], B.R. Roberts[19], S.S. Roberts[195], D. Robinson[46], M. Robles Manzano[151], A. Robson[86], A. Rocchi[114,115], C. Roda[110,111], S. Rodriguez Bosca[61], Y. Rodriguez Garcia[27], A.M. Rodríguez Vera[169], S. Roe[61], J.T. Roemer[61], O. Røhne[178], R.A. Rojas[61], C.P.A. Roland[180], J. Roloff[43], A. Romaniouk[120], E. Romano[108,109], M. Romano[30], A.C. Romero Hernandez[234], N. Rompotis[143], L. Roos[180], S. Rosati[112], B.J. Rosser[64], E. Rossi[179], E. Rossi[106,107], L.P. Rossi[88], L. Rossini[80], R. Rosten[172], M. Rotaru[35], R. Roth[61], B. Rottler[80], D. Rousseau[96], D. Rousso[74], S. Roy-Garand[226], A. Rozanov[153], Z. M. A. Rozario[86], Y. Rozen[221], A. Rubio Jimenez[235], V.H. Ruelas Rivera[21], T.A. Ruggeri[1], A. Ruggiero[179], A. Ruiz-Martinez[235], A. Rummler[61], Z. Rurikova[80], N.A. Rusakovich[63], H.L. Russell[237], G. Russo[112,113], J.P. Rutherfoord[8], S. Rutherford Colmenares[46], M. Rybar[192], P. Rybczynski[135], E.B. Rye[178], A. Ryzhov[70], J.A. Sabater Iglesias[82], H.F-W. Sadrozinski[195], F. Safai Tehrani[112], S. Saha[1], M. Sahinsoy[123], B. Sahoo[241], A. Saibel[235], B. T. Saifuddin[173], M. Saimpert[194], G.T. Saito[126], M. Saito[224], T. Saito[224], A. Sala[104,105], D. Salamani[61], A. Salnikov[212], J. Salt[235], A. Salvador Salas[222], D. Salvatore[69,68], F. Salvatore[215], A. Salzburger[61], D. Sammel[80], E. Sampson[142], D. Sampsonidis[V,223], D. Sampsonidou[176], J. Sánchez[235], V. Sanchez Sebastian[235], H. Sandaker[178], C.O. Sander[74], J.A. Sandesara[242], M. Sandhoff[243], C. Sandoval[28], L. Sanfilippo[90], D.P.C. Sankey[193], T. Sano[138], A. Sansoni[79], L. Santi[61], C. Santoni[65], H. Santos[183,184], A. Santra[241], E. Sanzani[30,29], K.A. Saoucha[133], J.G. Saraiva[183,186], J. Sardain[8], O. Sasaki[129], K. Sato[229], C. Sauer[61], E. Sauvan[5], P. Savard[XXXVII,226], R. Sawada[224], C. Sawyer[193], L. Sawyer[148], C. Sbarra[30], A. Sbrizzi[30,29], T. Scanlon[147], J. Schaarschmidt[203], U. Schäfer[151], A.C. Schaffer[96,70], D. Schaile[160], R.D. Schamberger[214], C. Scharf[21], M.M. Schefer[22], V.A. Schegelsky[62], D. Scheirich[192], M. Schernau[200], C. Scheulen[82], C. Schiavi[84,83], M. Schioppa[69,68], B. Schlag[212], S. Schlenker[61], J. Schmeing[243], M. A. Schmidt[243], K. Schmieden[151], C. Schmitt[151], N. Schmitt[151], S. Schmitt[74], L. Schoeffel[194], A. Schoening[91], P.G. Scholer[54], E. Schopf[210], M. Schott[31], S. Schramm[82], T. Schroer[82], H-C. Schultz-Coulon[90], M. Schumacher[80], B.A. Schumm[195], Ph. Schune[194], H.R. Schwartz[195], A. Schwartzman[212], T.A. Schwarz[157], Ph. Schwemling[194], R. Schwienhorst[158], F.G. Sciacca[22], A. Sciandra[43], G. Sciolla[33], F. Scuri[110], C.D. Sebastiani[61], K. Sedlaczek[169], S.C. Seidel[166], A. Seiden[195], B.D. Seidlitz[66], C. Seitz[74], J.M. Seixas[125], G. Sekhniaidze[106], L. Selem[87], N. Semprini-Cesari[30,29], A. Semushin[245,62], D. Sengupta[82], V. Senthilkumar[235], L. Serin[96], M. Sessa[114,115], H. Severini[173], F. Sforza[84,83], A. Sfyrla[82], Q. Sha[15], E. Shabalina[81], H. Shaddix[169], A.H. Shah[46], R. Shaheen[213], J.D. Shahinian[181], D. Shaked Renous[241], M. Shamim[61], L.Y. Shan[15], M. Shapiro[19], A. Sharma[61], A.S. Sharma[236], P. Sharma[43], P.B. Shatalov[62], K. Shaw[215], S.M. Shaw[152], Q. Shen[15], D.J. Sheppard[211], P. Sherwood[147], L. Shi[147], X. Shi[15], S. Shimizu[129], C.O. Shimmin[244], I.P.J. Shipsey[XLV,179], S. Shirabe[139], M. Shiyakova[XXVIII,63], M.J. Shochet[64], D.R. Shope[178], B. Shrestha[173], S. Shrestha[XLIII,172], I. Shreyber[63], M.J. Shroff[237], P. Sicho[190], A.M. Sickles[234], E. Sideras Haddad[53,232], A. C. Sidley[168], A. Sidoti[30], F. Siegert[76], Dj. Sijacki[17], F. Sili[141], J.M. Silva[78], I. Silva Ferreira[125], M.V. Silva Oliveira[43], S.B. Silverstein[72], S. Simion[96], R. Simoniello[61], E.L. Simpson[152], H. Simpson[215], L.R. Simpson[157], S. Simsek[123], S. Sindhu[81], P. Sinervo[226], S. N. Singh[33], S. Singh[43], S. Sinha[74], S. Sinha[152], M. Sioli[30,29], K. Sioulas[10], I. Siral[61], E. Sitnikova[74], J. Sjölin[72,73], A. Skaf[81], E. Skorda[23], P. Skubic[173], M. Slawinska[137], I. Slazyk[18], V. Smakhtin[241], B.H. Smart[193], S.Yu. Smirnov[197], Y. Smirnov[123], L.N. Smirnova[I,62], O. Smirnova[149], A.C. Smith[66], D.R. Smith[231], E.A. Smith[64], J.L. Smith[152], M. B. Smith[54], R. Smith[212], H. Smitmanns[151], M. Smizanska[142], K. Smolek[191], P. Smolyanskiy[191], A.A. Snesarev[63], H.L. Snoek[168], S. Snyder[43], R. Sobie[XXX,237], A. Soffer[222], C.A. Solans Sanchez[61], E.Yu. Soldatov[63], U. Soldevila[235], A.A. Solodkov[53], S. Solomon[33], A. Soloshenko[63], K. Solovieva[80], O.V. Solovyanov[65], P. Sommer[76], A. Sonay[14], W.Y. Song[228], A. Sopczak[191], A.L. Sopio[78], F. Sopkova[42], J. D. Sorenson[166], I.R. Sotarriva Alvarez[202], V. Sothilingam[90], O. J. Soto Sandoval[198,197], S. Sottocornola[98], R. Soualah[130], Z. Soumaimi[59], D. South[74], N. Soybelman[241], S. Spagnolo[102,103], M. Spalla[161], D. Sperlich[80], B. Spisso[106,107], D.P. Spiteri[86], L. Splendori[153], M. Spousta[192], E.J. Staats[54], R. Stamen[90], E. Stanecka[137], W. Stanek-Maslouska[74], M.V. Stange[76], B. Stanislaus[19], M.M. Stanitzki[74], B. Stapf[74], E.A. Starchenko[62], G.H. Stark[195], J. Stark[140], P. Staroba[190], P. Starovoitov[133], R. Staszewski[137], G. Stavropoulos[71], A. Stefl[61], P. Steinberg[43], B. Stelzer[211,227], H.J. Stelzer[182], O. Stelzer[227], H. Stenzel[85], T.J. Stevenson[215], G.A. Stewart[61], J.R. Stewart[174], M.C. Stockton[61], G. Stoicea[35], M. Stolarski[183], S. Stonjek[161], A. Straessner[76], J. Strandberg[213], S. Strandberg[72,73], M. Stratmann[243], M. Strauss[173], T. Strebler[153], P. Strizenec[42], R. Ströhmer[238], D.M. Strom[176], R. Stroynowski[70], A. Strubig[72,73], S.A. Stucci[43], B. Stugu[18], J. Stupak[173], N.A. Styles[74], D. Su[212], S. Su[89], W. Su[207], X. Su[89], D. Suchy[41], K. Sugizaki[181], V.V. Sulin[62], M.J. Sullivan[143], D.M.S. Sultan[179], L. Sultanaliyeva[62], S. Sultansoy[4], S. Sun[242], W. Sun[15], O. Sunneborn Gudnadottir[233], N. Sur[149], M.R. Sutton[215], H. Suzuki[229], M. Svatos[190], P. N. Swallow[46], M. Swiatlowski[227], T. Swirski[238], I. Sykora[41], M. Sykora[192], T. Sykora[192], D. Ta[151],

K. Tackmann[XXVII,74], A. Taffard[231], R. Tafirout[227], Y. Takubo[129], M. Talby[153], A.A. Talyshev[62], K.C. Tam[93], N.M. Tamir[222], A. Tanaka[224], J. Tanaka[224], R. Tanaka[96], M. Tanasini[214], Z. Tao[236], S. Tapia Araya[201], S. Tapprogge[151], A. Tarek Abouelfadl Mohamed[158], S. Tarem[221], K. Tariq[15], G. Tarna[35], G.F. Tartarelli[104], M. J. Tartarin[140], P. Tas[192], M. Tasevsky[190], E. Tassi[69,68], A.C. Tate[234], G. Tateno[224], Y. Tayalati[XXIX,59], G.N. Taylor[156], W. Taylor[228], A.S. Tegetmeier[140], P. Teixeira-Dias[146], J.J. Teoh[226], K. Terashi[224], J. Terron[150], S. Terzo[14], M. Testa[79], R.J. Teuscher[XXX,226], A. Thaler[120], O. Theiner[82], T. Theveneaux-Pelzer[153], O. Thielmann[243], D.W. Thomas[146], J.P. Thomas[23], E.A. Thompson[19], P.D. Thompson[23], E. Thomson[181], R. E. Thornberry[70], C. Tian[89], Y. Tian[82], V. Tikhomirov[123], Yu.A. Tikhonov[63], S. Timoshenko[62], D. Timoshyn[192], E.X.L. Ting[1], P. Tipton[244], A. Tishelman-Charny[43], S.H. Tlou[53], K. Todome[202], S. Todorova-Nova[192], S. Todt[76], L. Toffolin[99,101], M. Togawa[129], J. Tojo[139], S. Tokár[41], O. Toldaiev[98], G. Tolkachev[153], M. Tomoto[129,162], L. Tompkins[XVII,212], E. Torrence[176], H. Torres[140], E. Torró Pastor[235], M. Toscani[44], C. Tosciri[64], M. Tost[12], D.R. Tovey[208], T. Trefzger[238], P.M. Tricarico[14], A. Tricoli[43], I.M. Trigger[227], S. Trincaz-Duvoid[180], D.A. Trischuk[33], A. Tropina[63], L. Truong[49], M. Trzebinski[137], A. Trzupek[137], F. Tsai[214], M. Tsai[157], A. Tsiamis[223], P.V. Tsiareshka[63], S. Tsigaridas[227], A. Tsirigotis[XXIII,223], V. Tsiskaridze[226], E.G. Tskhadadze[218], M. Tsopoulou[223], Y. Tsujikawa[138], I.I. Tsukerman[62], V. Tsulaia[19], S. Tsuno[129], K. Tsuri[171], D. Tsybychev[214], Y. Tu[93], A. Tudorache[35], V. Tudorache[35], S. Turchikhin[84,83], I. Turk Cakir[3], R. Turra[104], T. Turtuvshin[XXXI,63], P.M. Tuts[66], S. Tzamarias[V,223], E. Tzovara[151], Y. Uematsu[129], F. Ukegawa[229], P.A. Ulloa Poblete[198,197], E.N. Umaka[43], G. Unal[61], A. Undrus[43], G. Unel[231], J. Urban[42], P. Urrejola[196], G. Usai[9], R. Ushioda[225], M. Usman[159], F. Ustuner[78], Z. Uysal[123], V. Vacek[191], B. Vachon[155], T. Vafeiadis[61], A. Vaitkus[147], C. Valderanis[160], E. Valdes Santurio[72,73], M. Valente[227], S. Valentinetti[30,29], A. Valero[235], E. Valiente Moreno[235], A. Vallier[140], J.A. Valls Ferrer[235], D. R. Van Arneman[168], T.R. Van Daalen[203], A. Van Der Graaf[75], H. Z. Van Der Schyf[53], P. Van Gemmeren[7], M. Van Rijnbach[61], S. Van Stroud[147], I. Van Vulpen[168], P. Vana[192], M. Vanadia[114,115], U. M. Vande Voorde[213], W. Vandelli[61], E.R. Vandewall[174], D. Vannicola[222], L. Vannoli[79], R. Vari[112], E.W. Varnes[8], C. Varni[20], D. Varouchas[96], L. Varriale[235], K.E. Varvell[216], M.E. Vasile[35], L. Vaslin[129], M. D. Vassilev[212], A. Vasyukov[63], L. M. Vaughan[174], R. Vavricka[192], T. Vazquez Schroeder[14], J. Veatch[45], V. Vecchio[152], M.J. Veen[154], I. Veliscek[43], I. Velkovska[144], L.M. Veloce[226], F. Veloso[183,185], S. Veneziano[112], A. Ventura[102,103], S. Ventura Gonzalez[194], A. Verbytskyi[161], M. Verducci[110,111], C. Vergis[145], M. Verissimo De Araujo[125], W. Verkerke[168], J.C. Vermeulen[168], C. Vernieri[212], M. Vessella[231], M.C. Vetterli[XXXVII,211], A. Vgenopoulos[151], N. Viaux Maira[201], T. Vickey[208], O.E. Vickey Boeriu[208], G.H.A. Viehhauser[179], L. Vigani[91], M. Vigl[161], M. Villa[30,29], M. Villaplana Perez[235], E.M. Villhauer[78], E. Vilucchi[79], M.G. Vincter[54], A. Visibile[168], C. Vittori[61], I. Vivarelli[30,29], E. Voevodina[161], F. Vogel[160], J.C. Voigt[76], P. Vokac[191], Yu. Volkotrub[136], E. Von Toerne[31], B. Vormwald[61], K. Vorobev[77], M. Vos[235], K. Voss[210], M. Vozak[61], L. Vozdecky[173], N. Vranjes[17], M. Vranjes Milosavljevic[17], M. Vreeswijk[168], N.K. Vu[207,206], R. Vuillermet[61], O. Vujinovic[151], I. Vukotic[64], I. K. Vyas[54], J.F. Wack[46], S. Wada[229], C. Wagner[212], J.M. Wagner[19], W. Wagner[243], S. Wahdan[243], H. Wahlberg[141], C. H. Waits[173], J. Walder[193], R. Walker[160], W. Walkowiak[210], A. Wall[181], E.J. Wallin[149], T. Wamorkar[19], A.Z. Wang[195], C. Wang[151], C. Wang[12], H. Wang[19], J. Wang[94], P. Wang[152], P. Wang[147], R. Wang[88], R. Wang[7], S.M. Wang[217], S. Wang[15], T. Wang[89], T. Wang[89], W.T. Wang[121], W. Wang[15], X. Wang[234], X. Wang[206], X. Wang[74], Y. Wang[163], Y. Wang[89], Z. Wang[157], Z. Wang[207,77,206], Z. Wang[157], C. Wanotayaroj[129], A. Warburton[155], A.L. Warnerbring[210], N. Warrack[86], S. Waterhouse[146], A.T. Watson[23], H. Watson[78], M.F. Watson[23], E. Watton[86], G. Watts[203], B.M. Waugh[147], J. M. Webb[80], C. Weber[43], H. A. Weber[21], M.S. Weber[22], S.M. Weber[90], C. Wei[89], Y. Wei[80], A.R. Weidberg[179], E.J. Weik[170], J. Weingarten[75], C. Weiser[80], C.J. Wells[74], T. Wenaus[43], B. Wendland[75], T. Wengler[61], N.S. Wenke[161], N. Wermes[31], M. Wessels[90], A.M. Wharton[142], A.S. White[88], A. White[9], M.J. White[1], D. Whiteson[231], L. Wickremasinghe[177], W. Wiedenmann[242], M. Wielers[193], R. Wierda[213], C. Wiglesworth[67], H.G. Wilkens[61], J. J. H. Wilkinson[46], D.M. Williams[66], H.H. Williams[181], S. Williams[46], S. Willocq[154], B.J. Wilson[152], D.J. Wilson[152], P.J. Windischhofer[64], F.I. Winkel[44], F. Winklmeier[176], B.T. Winter[80], M. Wittgen[212], M. Wobisch[148], T. Wojtkowski[87], Z. Wolffs[168], J. Wollrath[61], M.W. Wolter[137], H. Wolters[183,185], M.C. Wong[195], E.L. Woodward[66], S.D. Worm[74], B.K. Wosiek[137], K.W. Woźniak[137], S. Wozniewski[81], K. Wraight[86], C. Wu[226], C. Wu[23], M. Wu[164], M. Wu[167], S.L. Wu[242], S. Wu[15], X. Wu[82], X. Wu[89], Y. Wu[89], Z. Wu[5], J. Wuerzinger[XXXV,161], T.R. Wyatt[152], B.M. Wynne[78], S. Xella[67], L. Xia[163], M. Xia[16], M. Xie[89], A. Xiong[176], J. Xiong[19], D. Xu[15], H. Xu[89], L. Xu[89], R. Xu[181], T. Xu[157], Y. Xu[203], Z. Xu[78], Z. Xu[163], B. Yabsley[216], S. Yacoob[47], Y. Yamaguchi[129], E. Yamashita[224], H. Yamauchi[229], T. Yamazaki[19], Y. Yamazaki[134], S. Yan[86], Z. Yan[154], H.J. Yang[206,207], H.T. Yang[89], S. Yang[89], T. Yang[94], X. Yang[61], X. Yang[15], Y. Yang[224], Y. Yang[89], W-M. Yao[19], C. L. Yardley[215], H. Ye[81], J. Ye[15], S. Ye[43], X. Ye[89], Y. Yeh[147], I. Yeletskikh[63], B. Yeo[20], M.R. Yexley[147], T. P. Yildirim[179], P. Yin[66], K. Yorita[240], C.J.S. Young[61], C. Young[212], N.D. Young[176], Y. Yu[89], J. Yuan[XXXIX,15,165], M. Yuan[157], R. Yuan[207,206], L. Yue[147], M. Zaazoua[89], B. Zabinski[137], I. Zahir[55], A. Zaio[84,83], Z.K. Zak[137], T. Zakareishvili[235], S. Zambito[82], J.A. Zamora Saa[199], J. Zang[224], D. Zanzi[80], R. Zanzottera[104,105], O. Zaplatilek[191], C. Zeitnitz[243], H. Zeng[15], J.C. Zeng[234], D.T. Zenger Jr[33], O. Zenin[62], T. Ženiš[41], S. Zenz[145], D. Zerwas[96], M. Zhai[15,165], D.F. Zhang[208], J. Zhang[204], J. Zhang[7], K. Zhang[15,165], L. Zhang[89], L. Zhang[163], P. Zhang[15,165], R. Zhang[242], S. Zhang[140], T. Zhang[224], X. Zhang[206], Y. Zhang[203], Y. Zhang[147], Y. Zhang[89], Y. Zhang[163], Z. Zhang[19], Z. Zhang[204], Z. Zhang[96], H. Zhao[203], T. Zhao[204], Y. Zhao[54], Z. Zhao[89], Z. Zhao[89], A. Zhemchugov[63], J. Zheng[163], K. Zheng[234], X. Zheng[89], Z. Zheng[212], D. Zhong[234], B. Zhou[157], H. Zhou[8], N. Zhou[206], Y. Zhou[16], Y. Zhou[163], Y. Zhou[8], C.G. Zhu[204], J. Zhu[157], X. Zhu[207], Y. Zhu[206], Y. Zhu[89], X. Zhuang[15], K. Zhukov[98], N.I. Zimine[63], J. Zinsser[91], M. Ziolkowski[210], L. Živković[17], A. Zoccoli[30,29], K. Zoch[88], T.G. Zorbas[208], O. Zormpa[71], W. Zou[66], L. Zwalinski[61]

Affiliation Notes

[I] Also at Affiliated with an institute formerly covered by a cooperation agreement with CERN
[II] Also at An-Najah National University, Nablus, Palestine
[III] Also at Borough of Manhattan Community College, City University of New York, New York NY, United States of America
[IV] Also at Center for High Energy Physics, Peking University, China
[V] Also at Center for Interdisciplinary Research and Innovation (CIRI-AUTH), Thessaloniki, Greece
[VI] Also at Centre of Physics of the Universities of Minho and Porto (CF-UM-UP), Portugal
[VII] Also at CERN, Geneva, Switzerland
[VIII] Also at CMD-AC UNEC Research Center, Azerbaijan State University of Economics (UNEC), Azerbaijan
[IX] Also at Département de Physique Nucléaire et Corpusculaire, Université de Genève, Genève, Switzerland
[X] Also at Departament de Fisica de la Universitat Autonoma de Barcelona, Barcelona, Spain

[XI] Also at Department of Financial and Management Engineering, University of the Aegean, Chios, Greece
[XII] Also at Department of Mathematical Sciences, University of South Africa, Johannesburg, South Africa
[XIII] Also at Department of Modern Physics and State Key Laboratory of Particle Detection and Electronics, University of Science and Technology of China, Hefei, China
[XIV] Also at Department of Physics, Bolu Abant Izzet Baysal University, Bolu, Türkiye
[XV] Also at Department of Physics, California State University, Sacramento, United States of America
[XVI] Also at Department of Physics, King's College London, London, United Kingdom
[XVII] Also at Department of Physics, Stanford University, Stanford CA, United States of America
[XVIII] Also at Department of Physics, Stellenbosch University, South Africa
[XIX] Also at Department of Physics, University of Fribourg, Fribourg, Switzerland
[XX] Also at Department of Physics, University of Thessaly, Greece
[XXI] Also at Department of Physics, Westmont College, Santa Barbara, United States of America
[XXII] Also at Faculty of Physics, Sofia University, 'St. Kliment Ohridski', Sofia, Bulgaria
[XXIII] Also at Hellenic Open University, Patras, Greece
[XXIV] Also at Henan University, China
[XXV] Also at Imam Mohammad Ibn Saud Islamic University, Saudi Arabia
[XXVI] Also at Institucio Catalana de Recerca i Estudis Avancats, ICREA, Barcelona, Spain
[XXVII] Also at Institut für Experimentalphysik, Universität Hamburg, Hamburg, Germany
[XXVIII] Also at Institute for Nuclear Research and Nuclear Energy (INRNE) of the Bulgarian Academy of Sciences, Sofia, Bulgaria
[XXIX] Also at Institute of Applied Physics, Mohammed VI Polytechnic University, Ben Guerir, Morocco
[XXX] Also at Institute of Particle Physics (IPP), Canada
[XXXI] Also at Institute of Physics and Technology, Mongolian Academy of Sciences, Ulaanbaatar, Mongolia
[XXXII] Also at Institute of Physics, Azerbaijan Academy of Sciences, Baku, Azerbaijan
[XXXIII] Also at Institute of Theoretical Physics, Ilia State University, Tbilisi, Georgia
[XXXIV] Also at National Institute of Physics, University of the Philippines Diliman (Philippines), Philippines
[XXXV] Also at Technical University of Munich, Munich, Germany
[XXXVI] Also at The Collaborative Innovation Center of Quantum Matter (CICQM), Beijing, China
[XXXVII] Also at TRIUMF, Vancouver BC, Canada
[XXXVIII] Also at Università di Napoli Parthenope, Napoli, Italy
[XXXIX] Also at University of Chinese Academy of Sciences (UCAS), Beijing, China
[XL] Also at University of Colorado Boulder, Department of Physics, Colorado, United States of America
[XLI] Also at University of Siena, Italy
[XLII] Also at University of the Western Cape, South Africa
[XLIII] Also at Washington College, Chestertown, MD, United States of America
[XLIV] Also at Yeditepe University, Physics Department, Istanbul, Türkiye
[XLV] Deceased

Collaboration Institutes

[1] Department of Physics, University of Adelaide, Adelaide, Australia
[2] Department of Physics, University of Alberta, Edmonton, AB, Canada
[3] Department of Physics, Ankara University, Ankara, Türkiye
[4] Division of Physics, TOBB University of Economics and Technology, Ankara, Türkiye
[5] LAPP, Université Savoie Mont Blanc, CNRS/IN2P3, Annecy, France
[6] APC, Université Paris Cité, CNRS/IN2P3, Paris, France
[7] High Energy Physics Division, Argonne National Laboratory, Argonne, IL, United States of America
[8] Department of Physics, University of Arizona, Tucson, AZ, United States of America
[9] Department of Physics, University of Texas at Arlington, Arlington, TX, United States of America
[10] Physics Department, National and Kapodistrian University of Athens, Athens, Greece
[11] Physics Department, National Technical University of Athens, Zografou, Greece
[12] Department of Physics, University of Texas at Austin, Austin, TX, United States of America
[13] Institute of Physics, Azerbaijan Academy of Sciences, Baku, Azerbaijan
[14] Institut de Física d'Altes Energies (IFAE), Barcelona Institute of Science and Technology, Barcelona, Spain
[15] Institute of High Energy Physics, Chinese Academy of Sciences, Beijing, China
[16] Physics Department, Tsinghua University, Beijing, China
[17] Institute of Physics, University of Belgrade, Belgrade, Serbia
[18] Department for Physics and Technology, University of Bergen, Bergen, Norway
[19] Physics Division, Lawrence Berkeley National Laboratory, Berkeley, CA, United States of America
[20] University of California, Berkeley, CA, United States of America
[21] Institut für Physik, Humboldt Universität zu Berlin, Berlin, Germany
[22] Albert Einstein Center for Fundamental Physics and Laboratory for High Energy Physics, University of Bern, Bern, Switzerland
[23] School of Physics and Astronomy, University of Birmingham, Birmingham, United Kingdom
[24] Department of Physics, Bogazici University, Istanbul, Türkiye
[25] Department of Physics Engineering, Gaziantep University, Gaziantep, Türkiye
[26] Department of Physics, Istanbul University, Istanbul, Türkiye
[27] Facultad de Ciencias y Centro de Investigaciónes, Universidad Antonio Nariño, Bogotá, Colombia
[28] Departamento de Física, Universidad Nacional de Colombia, Bogotá, Colombia
[29] Dipartimento di Fisica e Astronomia A. Righi, Università di Bologna, Bologna, Italy
[30] INFN Sezione di Bologna, Italy
[31] Physikalisches Institut, Universität Bonn, Bonn, Germany
[32] Department of Physics, Boston University, Boston, MA, United States of America
[33] Department of Physics, Brandeis University, Waltham, MA, United States of America
[34] Transilvania University of Brasov, Brasov, Romania
[35] Horia Hulubei National Institute of Physics and Nuclear Engineering, Bucharest, Romania
[36] Department of Physics, Alexandru Ioan Cuza University of Iasi, Iasi, Romania
[37] Physics Department, National Institute for Research and Development of Isotopic and Molecular Technologies, Cluj-Napoca, Romania
[38] National University of Science and Technology Politechnica, Bucharest, Romania
[39] West University in Timisoara, Timisoara, Romania
[40] Faculty of Physics, University of Bucharest, Bucharest, Romania
[41] Faculty of Mathematics, Physics and Informatics, Comenius University, Bratislava, Slovak Republic
[42] Department of Subnuclear Physics, Institute of Experimental Physics, Slovak Academy of Sciences, Kosice, Slovak Republic
[43] Physics Department, Brookhaven National Laboratory, Upton, NY, United States of America

[44] Facultad de Ciencias Exactas y Naturales, Departamento de Física, Instituto de Física de Buenos Aires (IFIBA), CONICET, Universidad de Buenos Aires, Buenos Aires, Argentina
[45] California State University, CA, United States of America
[46] Cavendish Laboratory, University of Cambridge, Cambridge, United Kingdom
[47] Department of Physics, University of Cape Town, Cape Town, South Africa
[48] iThemba Labs, Western Cape, South Africa
[49] Department of Mechanical Engineering Science, University of Johannesburg, Johannesburg, South Africa
[50] National Institute of Physics, University of the Philippines Diliman (Philippines), Philippines
[51] Department of Physics, University of South Africa, Pretoria, South Africa
[52] University of Zululand, KwaDlangezwa, South Africa
[53] School of Physics, University of the Witwatersrand, Johannesburg, South Africa
[54] Department of Physics, Carleton University, Ottawa, ON, Canada
[55] Faculté des Sciences Ain Chock, Université Hassan II de Casablanca, Morocco
[56] Faculté des Sciences, Université Ibn-Tofail, Kénitra, Morocco
[57] Faculté des Sciences Semlalia, Université Cadi Ayyad, LPHEA-Marrakech, Morocco
[58] Faculté des Sciences, LPMR, Université Mohamed Premier, Oujda, Morocco
[59] Faculté des sciences, Université Mohammed V, Rabat, Morocco
[60] Institute of Applied Physics, Mohammed VI Polytechnic University, Ben Guerir, Morocco
[61] CERN, Geneva, Switzerland
[62] Affiliated with an institute formerly covered by a cooperation agreement with CERN
[63] Affiliated with an international laboratory covered by a cooperation agreement with CERN
[64] Enrico Fermi Institute, University of Chicago, Chicago, IL, United States of America
[65] LPC, Université Clermont Auvergne, CNRS/IN2P3, Clermont-Ferrand, France
[66] Nevis Laboratory, Columbia University, Irvington, NY, United States of America
[67] Niels Bohr Institute, University of Copenhagen, Copenhagen, Denmark
[68] Dipartimento di Fisica, Università della Calabria, Rende, Italy
[69] INFN Gruppo Collegato di Cosenza, Laboratori Nazionali di Frascati, Italy
[70] Physics Department, Southern Methodist University, Dallas, TX, United States of America
[71] National Centre for Scientific Research Demokritos, Agia Paraskevi, Greece
[72] Department of Physics, Stockholm University, Sweden
[73] Oskar Klein Centre, Stockholm, Sweden
[74] Deutsches Elektronen-Synchrotron DESY, Hamburg and Zeuthen, Germany
[75] Fakultät Physik, Technische Universität Dortmund, Dortmund, Germany
[76] Institut für Kern- und Teilchenphysik, Technische Universität Dresden, Dresden, Germany
[77] Department of Physics, Duke University, Durham, NC, United States of America
[78] SUPA - School of Physics and Astronomy, University of Edinburgh, Edinburgh, United Kingdom
[79] INFN e Laboratori Nazionali di Frascati, Frascati, Italy
[80] Physikalisches Institut, Albert-Ludwigs-Universität Freiburg, Freiburg, Germany
[81] II. Physikalisches Institut, Georg-August-Universität Göttingen, Göttingen, Germany
[82] Département de Physique Nucléaire et Corpusculaire, Université de Genève, Genève, Switzerland
[83] Dipartimento di Fisica, Università di Genova, Genova, Italy
[84] INFN Sezione di Genova, Italy
[85] II. Physikalisches Institut, Justus-Liebig-Universität Giessen, Giessen, Germany
[86] SUPA - School of Physics and Astronomy, University of Glasgow, Glasgow, United Kingdom
[87] LPSC, Université Grenoble Alpes, CNRS/IN2P3, Grenoble INP, Grenoble, France
[88] Laboratory for Particle Physics and Cosmology, Harvard University, Cambridge, MA, United States of America
[89] Department of Modern Physics and State Key Laboratory of Particle Detection and Electronics, University of Science and Technology of China, Hefei, China
[90] Kirchhoff-Institut für Physik, Ruprecht-Karls-Universität Heidelberg, Heidelberg, Germany
[91] Physikalisches Institut, Ruprecht-Karls-Universität Heidelberg, Heidelberg, Germany
[92] Department of Physics, Chinese University of Hong Kong, Shatin Hong Kong, N.T, China
[93] Department of Physics, University of Hong Kong, Hong Kong, China
[94] Department of Physics, Institute for Advanced Study, Hong Kong University of Science and Technology, Clear Water Bay, Kowloon Hong Kong, China
[95] Department of Physics, National Tsing Hua University, Hsinchu, Taiwan
[96] IJCLab, Université Paris-Saclay, CNRS/IN2P3, Orsay, 91405, France
[97] Centro Nacional de Microelectrónica (IMB-CNM-CSIC), Barcelona, Spain
[98] Department of Physics, Indiana University, Bloomington, IN, United States of America
[99] INFN Gruppo Collegato di Udine, Sezione di Trieste, Udine, Italy
[100] ICTP, Trieste, Italy
[101] Dipartimento Politecnico di Ingegneria e Architettura, Università di Udine, Udine, Italy
[102] INFN Sezione di Lecce, Italy
[103] Dipartimento di Matematica e Fisica, Università del Salento, Lecce, Italy
[104] INFN Sezione di Milano, Italy
[105] Dipartimento di Fisica, Università di Milano, Milano, Italy
[106] INFN Sezione di Napoli, Italy
[107] Dipartimento di Fisica, Università di Napoli, Napoli, Italy
[108] INFN Sezione di Pavia, Italy
[109] Dipartimento di Fisica, Università di Pavia, Pavia, Italy
[110] INFN Sezione di Pisa, Italy
[111] Dipartimento di Fisica E. Fermi, Università di Pisa, Pisa, Italy
[112] INFN Sezione di Roma, Italy
[113] Dipartimento di Fisica, Sapienza Università di Roma, Roma, Italy
[114] INFN Sezione di Roma Tor Vergata, Italy
[115] Dipartimento di Fisica, Università di Roma Tor Vergata, Roma, Italy
[116] INFN Sezione di Roma Tre, Italy
[117] Dipartimento di Matematica e Fisica, Università Roma Tre, Roma, Italy
[118] INFN-TIFPA, Italy
[119] Università degli Studi di Trento, Trento, Italy
[120] Department of Astro and Particle Physics, Universität Innsbruck, Innsbruck, Austria
[121] University of Iowa, Iowa City, IA, United States of America
[122] Department of Physics and Astronomy, Iowa State University, Ames, IA, United States of America
[123] Istinye University, Sariyer, Istanbul, Türkiye
[124] Departamento de Engenharia Elétrica, Universidade Federal de Juiz de Fora (UFJF), Juiz de Fora, Brazil
[125] COPPE/EE/IF, Universidade Federal do Rio, De JaneiroRio de Janeiro, Brazil

[126] Instituto de Física, Universidade de São Paulo, São Paulo, Brazil
[127] Janeiro State University, Rio de Janeiro, Brazil
[128] Federal University of Bahia, Bahia, Brazil
[129] KEK, High Energy Accelerator Research Organization, Tsukuba, Japan
[130] Khalifa University of Science and Technology, Abu Dhabi, United Arab Emirates
[131] New York University Abu Dhabi, Abu Dhabi, United Arab Emirates
[132] United Arab Emirates University, Al Ain, United Arab Emirates
[133] University of Sharjah, Sharjah, United Arab Emirates
[134] Graduate School of Science, Kobe University, Kobe, Japan
[135] Faculty of Physics and Applied Computer Science, AGH University of Krakow, Krakow, Poland
[136] Marian Smoluchowski Institute of Physics, Jagiellonian University, Krakow, Poland
[137] Institute of Nuclear Physics, Polish Academy of Sciences, Krakow, Poland
[138] Faculty of Science, Kyoto University, Kyoto, Japan
[139] Research Center for Advanced Particle Physics, Department of Physics, Kyushu University, Fukuoka, Japan
[140] L2IT, Université de Toulouse, CNRS/IN2P3, UPS, Toulouse, France
[141] Instituto de Física La Plata, Universidad Nacional de La Plata and CONICET, La Plata, Argentina
[142] Physics Department, Lancaster University, Lancaster, United Kingdom
[143] Oliver Lodge Laboratory, University of Liverpool, Liverpool, United Kingdom
[144] Department of Experimental Particle Physics, Department of Physics, Jožef Stefan Institute, University of Ljubljana, Ljubljana, Slovenia
[145] Department of Physics and Astronomy, Queen Mary University of London, London, United Kingdom
[146] Department of Physics, Royal Holloway University of London, Egham, United Kingdom
[147] Department of Physics and Astronomy, University College London, London, United Kingdom
[148] Louisiana Tech University, Ruston, LA, United States of America
[149] Fysiska institutionen, Lunds universitet, Lund, Sweden
[150] Departamento de Física Teorica C-15 and CIAFF, Universidad Autónoma de Madrid, Madrid, Spain
[151] Institut für Physik, Universität Mainz, Mainz, Germany
[152] School of Physics and Astronomy, University of Manchester, Manchester, United Kingdom
[153] CPPM, Aix-Marseille Université, CNRS/IN2P3, Marseille, France
[154] Department of Physics, University of Massachusetts, Amherst, MA, United States of America
[155] Department of Physics, McGill University, Montreal, QC, Canada
[156] School of Physics, University of Melbourne, Victoria, Australia
[157] Department of Physics, University of Michigan, Ann Arbor, MI, United States of America
[158] Department of Physics and Astronomy, Michigan State University, East Lansing, MI, United States of America
[159] Group of Particle Physics, University of Montreal, Montreal, QC, Canada
[160] Fakultät für Physik, Ludwig-Maximilians-Universität München, München, Germany
[161] Max-Planck-Institut für Physik (Werner-Heisenberg-Institut), München, Germany
[162] Graduate School of Science and Kobayashi-Maskawa Institute, Nagoya University, Nagoya, Japan
[163] Department of Physics, Nanjing University, Nanjing, China
[164] School of Science, Shenzhen Campus of Sun Yat-sen University, China
[165] University of Chinese Academy of Science (UCAS), Beijing, China
[166] Department of Physics and Astronomy, University of New Mexico, Albuquerque, NM, United States of America
[167] Institute for Mathematics, Astrophysics and Particle Physics, Radboud University/Nikhef, Nijmegen, the Netherlands
[168] Nikhef National Institute for Subatomic Physics and University of Amsterdam, Amsterdam, the Netherlands
[169] Department of Physics, Northern Illinois University, DeKalb, IL, United States of America
[170] Department of Physics, New York University, New York, NY, United States of America
[171] Ochanomizu University, Bunkyo-ku, Otsuka Tokyo, Japan
[172] Ohio State University, Columbus, OH, United States of America
[173] Department of Physics and Astronomy, Homer L. Dodge, University of Oklahoma, Norman, OK, United States of America
[174] Department of Physics, Oklahoma State University, Stillwater, OK, United States of America
[175] Joint Laboratory of Optics, Palacký University, Olomouc, Czech Republic
[176] Institute for Fundamental Science, University of Oregon, Eugene, OR, United States of America
[177] Graduate School of Science, University of Osaka, Osaka, Japan
[178] Department of Physics, University of Oslo, Oslo, Norway
[179] Department of Physics, Oxford University, Oxford, United Kingdom
[180] LPNHE, Sorbonne Université, Université Paris Cité, CNRS/IN2P3, Paris, France
[181] Department of Physics, University of Pennsylvania, Philadelphia, PA, United States of America
[182] Department of Physics and Astronomy, University of Pittsburgh, Pittsburgh, PA, United States of America
[183] Laboratório de Instrumentação e Física Experimental de Partículas - LIP, Lisboa, Portugal
[184] Departamento de Física, Faculdade de Ciências, Universidade de Lisboa, Lisboa, Portugal
[185] Departamento de Física, Universidade de Coimbra, Coimbra, Portugal
[186] Centro de Física Nuclear da, Universidade de Lisboa, Lisboa, Portugal
[187] Departamento de Física, Escola de Ciências, Universidade do Minho, Braga, Portugal
[188] Departamento de Física Teórica y del Cosmos, Universidad de Granada, Granada, Spain, Spain
[189] Departamento de Física, Instituto Superior Técnico, Universidade de Lisboa, Lisboa, Portugal
[190] Institute of Physics, Czech Academy of Sciences, Prague, Czech Republic
[191] Czech Technical University, Prague Prague, Czech Republic
[192] Faculty of Mathematics and Physics, Charles University, Prague, Czech Republic
[193] Particle Physics Department, Rutherford Appleton Laboratory Didcot, United Kingdom
[194] IRFU, CEA, Université Paris-Saclay, Gif-sur-Yvette, France
[195] Santa Cruz Institute for Particle Physics, University of California Santa Cruz, Santa Cruz, CA, United States of America
[196] Departamento de Física, Pontificia Universidad Católica de Chile, Santiago, Chile
[197] Millennium Institute for Subatomic physics at high energy frontier (SAPHIR), Santiago, Chile
[198] Departamento de Física, Instituto de Investigación Multidisciplinario en Ciencia y Tecnología, Universidad de La Serena, Chile
[199] Department of Physics, Universidad Andres Bello, Santiago, Chile
[200] Instituto de Alta Investigación, Universidad de Tarapacá, Arica, Chile
[201] Departamento de Física, Universidad Técnica Federico Santa María, Valparaíso, Chile
[202] Department of Physics, Institute of Science, Tokyo, Japan
[203] Department of Physics, University of Washington, Seattle, WA, United States of America
[204] Institute of Frontier and Interdisciplinary Science and Key, Laboratory of Particle Physics and Particle Irradiation (MOE), Shandong University, Qingdao, China

[205] School of Physics, Zhengzhou University, China
[206] School of Physics and Astronomy, State Key Laboratory of Dark Matter Physics, Key Laboratory for Particle Astrophysics and Cosmology (MOE), Shanghai Jiao Tong University, SKLPPC, Shanghai, China
[207] State Key Laboratory of Dark Matter Physics, Tsung-Dao Lee Institute, Shanghai Jiao Tong University, Shanghai, China
[208] Department of Physics and Astronomy, University of Sheffield, Sheffield, United Kingdom
[209] Department of Physics, Shinshu University, Nagano, Japan
[210] Department Physik, Universität Siegen, Siegen, Germany
[211] Department of Physics, Simon Fraser University, Burnaby, BC, Canada
[212] SLAC National Accelerator Laboratory, Stanford, CA, United States of America
[213] Department of Physics, Royal Institute of Technology, Stockholm, Sweden
[214] Departments of Physics and Astronomy, Stony Brook University, Stony Brook, NY, United States of America
[215] Department of Physics and Astronomy, University of Sussex, Brighton, United Kingdom
[216] School of Physics, University of Sydney, Sydney, Australia
[217] Institute of Physics, Academia Sinica, Taipei, Taiwan
[218] E. Andronikashvili Institute of Physics, Iv. Javakhishvili, Tbilisi State University, Tbilisi, Georgia
[219] High Energy Physics Institute, Tbilisi State University, Tbilisi, Georgia
[220] University of Georgia, Tbilisi, Georgia
[221] Department of Physics, Israel Institute of Technology, Technion Haifa, Israel
[222] Beverly Sackler School of Physics and Astronomy, Tel Aviv University, Tel Aviv, Israel
[223] Department of Physics, Aristotle University of Thessaloniki, Thessaloniki, Greece
[224] International Center for Elementary Particle Physics, Department of Physics, University of Tokyo, Tokyo, Japan
[225] Graduate School of Science and Technology, Tokyo Metropolitan University, Tokyo, Japan
[226] Department of Physics, University of Toronto, Toronto, ON, Canada
[227] TRIUMF, Vancouver, BC, Canada
[228] Department of Physics and Astronomy, York University, Toronto, ON, Canada
[229] Division of Physics and Tomonaga Center, Faculty of Pure and Applied Sciences, the History of the Universe, University of Tsukuba, Tsukuba, Japan
[230] Department of Physics and Astronomy, Tufts University, Medford, MA, United States of America
[231] Department of Physics and Astronomy, University of California Irvine, Irvine, CA, United States of America
[232] University of West Attica, Athens, Greece
[233] Department of Physics and Astronomy, University of Uppsala, Uppsala, Sweden
[234] Department of Physics, University of Illinois, Urbana, IL, United States of America
[235] Centro Mixto, Instituto de Física Corpuscular (IFIC), Universidad de Valencia - CSIC, Valencia, Spain
[236] Department of Physics, University of British Columbia, Vancouver, BC, Canada
[237] Department of Physics and Astronomy, University of Victoria, Victoria, BC, Canada
[238] Fakultät für Physik und Astronomie, Julius-Maximilians-Universität Würzburg, Würzburg, Germany
[239] Department of Physics, University of Warwick, Coventry, United Kingdom
[240] Waseda University, Tokyo, Japan
[241] Department of Particle Physics and Astrophysics, Weizmann Institute of Science, Rehovot, Israel
[242] Department of Physics, University of Wisconsin, Madison, WI, United States of America
[243] Fachgruppe Physik, Fakultät für Mathematik und Naturwissenschaften, Bergische Universität Wuppertal, Wuppertal, Germany
[244] Department of Physics, Yale University, New Haven, CT, United States of America
[245] Yerevan Physics Institute, Yerevan, Armenia

References

[1] T. Han, Z. Si, K.M. Zurek, M.J. Strassler, Phenomenology of hidden valleys at hadron colliders, JHEP 07 (2008) 008. arXiv:0712.2041 [hep-ph], https://doi.org/10.1088/1126-6708/2008/07/008
[2] H. Dreiner, An introduction to explicit R-parity violation, Adv. Ser. Direct. High Energy Phys. 21 (2010) 565–583. arXiv:hep-ph/9707435, https://doi.org/10.1142/9789814307505_0017
[3] R. Barbier, et al., R-parity-violating supersymmetry, Phys. Rept. 420 (2005) 1–202. arXiv:hep-ph/0406039, https://doi.org/10.1016/j.physrep.2005.08.006
[4] C.R. Nappi, B.A. Ovrut, Supersymmetric extension of the SU(3) x SU(2) x U(1) model, Phys. Lett. B 113 (1982) 175. https://doi.org/10.1016/0370-2693(82)90418-X
[5] L. Alvarez-Gaumé, M. Claudson, M.B. Wise, Low-energy supersymmetry, Nucl. Phys. B 207 (1982) 96. https://doi.org/10.1016/0550-3213(82)90138-9
[6] M. Dine, W. Fischler, A phenomenological model of particle physics based on supersymmetry, Phys. Lett. B 110 (1982) 227. https://doi.org/10.1016/0370-2693(82)91241-2
[7] ATLAS Collaboration, The ATLAS experiment at the CERN large hadron collider, JINST 3 (2008) S08003. https://doi.org/10.1088/1748-0221/3/08/S08003
[8] L. Evans, P. Bryant, LHC machine, JINST 3 (2008) S08001. https://doi.org/10.1088/1748-0221/3/08/S08001
[9] ATLAS Collaboration, Search for displaced vertices of oppositely charged leptons from decays of long-lived particles in pp collisions at $\sqrt{s} = 13$ TeV with the ATLAS detector, Phys. Lett. B 801 (2020) 135114. arXiv:1907.10037 [hep-ex], https://doi.org/10.1016/j.physletb.2019.135114
[10] ATLAS Collaboration, Search for long-lived particles in final states with displaced dimuon vertices in pp collisions at $\sqrt{s} = 13$ TeV with the ATLAS detector, Phys. Rev. D 99 (2019) 012001. arXiv:1808.03057 [hep-ex], https://doi.org/10.1103/PhysRevD.99.012001
[11] ATLAS Collaboration, Search in diphoton and dielectron final states for displaced production of Higgs or Z bosons with the ATLAS detector in $\sqrt{s} = 13$ TeV pp collisions, Phys. Rev. D 108 (2023) 012012. arXiv:2304.12885 [hep-ex], https://doi.org/10.1103/PhysRevD.108.012012
[12] CMS Collaboration, Search for long-lived particles that decay into final states containing two electrons or two muons in proton–proton collisions at $\sqrt{s} = 8$ TeV, Phys. Rev. D 91 (2015) 052012. arXiv:1411.6977 [hep-ex], https://doi.org/10.1103/PhysRevD.91.052012
[13] CMS Collaboration, Search for inelastic dark matter in events with two displaced muons and missing transverse momentum in proton–proton collisions at $\sqrt{s} = 13$ TeV, Phys. Rev. Lett. 132 (2024) 041802. arXiv:2305.11649 [hep-ex], https://doi.org/10.1103/PhysRevLett.132.041802
[14] CMS Collaboration, Search for long-lived particles decaying into muon pairs in proton–proton collisions at $\sqrt{s} = 13$ TeV collected with a dedicated high-rate data stream, JHEP 04 (2022) 062. arXiv:2112.13769 [hep-ex], https://doi.org/10.1007/JHEP04(2022)062
[15] LHCb Collaboration, Searches for low-mass dimuon resonances, JHEP 2020 (10) (2020) 156. arXiv:2007.03923 [hep-ph], https://doi.org/10.1007/JHEP10(2020)156
[16] CMS Collaboration, Search for long-lived particles decaying to final states with a pair of muons in proton–proton collisions at $\sqrt{s} = 13.6$ TeV, JHEP 05 (2024) 047. arXiv:2402.14491 [hep-ex], https://doi.org/10.1007/JHEP05(2024)047
[17] ATLAS Collaboration, ATLAS Insertable B-Layer: Technical Design Report, 2010, https://cds.cern.ch/record/1291633.
[18] B. Abbott, et al., Production and integration of the ATLAS insertable B-layer, JINST 13 (2018) T05008. arXiv:1803.00844 [physics.ins-det], https://doi.org/10.1088/1748-0221/13/05/T05008
[19] G. Avoni, et al., The new LUCID-2 detector for luminosity measurement and monitoring in ATLAS, JINST 13 (2018) P07017. https://doi.org/10.1088/1748-0221/13/07/P07017
[20] ATLAS Collaboration, Performance of the ATLAS trigger system in 2015, Eur. Phys. J. C 77 (2017) 317. arXiv:1611.09661 [hep-ex], https://doi.org/10.1140/epjc/s10052-017-4852-3
[21] ATLAS Collaboration, Software and computing for Run 3 of the ATLAS experiment at the LHC, Eur. Phys. J. C 85 (2025) 234. arXiv:2404.06335 [hep-ex], https://doi.org/10.1140/epjc/s10052-024-13701-w
[22] Particle Data Group Collaboration, Particle Data Group, Review of particle physics, Phys. Rev. D 110 (3) (2024) 030001. https://doi.org/10.1103/PhysRevD.110.030001
[23] ATLAS Collaboration, Luminosity determination in pp collisions at $\sqrt{s} = 13$ TeV using the ATLAS detector at the LHC, Eur. Phys. J. C 83 (2023) 982. arXiv:2212.09379 [hep-ex], https://doi.org/10.1140/epjc/s10052-023-11747-w
[24] J. Alwall, R. Frederix, S. Frixione, V. Hirschi, F. Maltoni, O. Mattelaer, H.-S. Shao, T. Stelzer, P. Torrielli, M. Zaro, The automated computation of tree-level and next-to-leading order differential cross sections, and their matching to parton shower

simulations, JHEP 07 (2014) 079. arXiv:1405.0301 [hep-ph], https://doi.org/10.1007/JHEP07(2014)079
[25] T. Sjöstrand, S. Ask, J.R. Christiansen, R. Corke, N. Desai, P. Ilten, S. Mrenna, S. Prestel, C.O. Rasmussen, P.Z. Skands, An introduction to PYTHIA 8.2, Comput. Phys. Commun. 191 (2015) 159. arXiv:1410.3012 [hep-ph], https://doi.org/10.1016/j.cpc.2015.01.024
[26] ATLAS Collaboration, ATLAS Pythia 8 tunes to 7 TeV data, ATL-PHYS-PUB-2014-021, 2014. https://cds.cern.ch/record/1966419.
[27] NNPDF Collaboration, R.D. Ball, et al., Parton distributions for the LHC run II, JHEP 04 (2015) 040. arXiv:1410.8849 [hep-ex], https://doi.org/10.1007/JHEP04(2015)040
[28] S. Agostinelli, et al., Geant4 – a simulation toolkit, Nucl. Instrum. Meth. A 506 (2003) 250. https://doi.org/10.1016/S0168-9002(03)01368-8
[29] T. Sjöstrand, S. Mrenna, P. Skands, A brief introduction to PYTHIA 8.1, Comput. Phys. Commun. 178 (2008) 852–867. arXiv:0710.3820 [hep-ph], https://doi.org/10.1016/j.cpc.2008.01.036
[30] ATLAS Collaboration, The Pythia 8 A3 tune description of ATLAS minimum bias and inelastic measurements incorporating the Donnachie–Landshoff diffractive model, ATL-PHYS-PUB-2016-017, 2016. https://cds.cern.ch/record/2206965.
[31] S. Frixione, P. Nason, C. Oleari, Matching NLO QCD computations with parton shower simulations: the POWHEG method, JHEP 11 (2007) 070. arXiv:0709.2092 [hep-ph], https://doi.org/10.1088/1126-6708/2007/11/070
[32] S. Alioli, P. Nason, C. Oleari, E. Re, NLO vector-boson production matched with shower in POWHEG, JHEP 07 (2008) 060. arXiv:0805.4802 [hep-ph], https://doi.org/10.1088/1126-6708/2008/07/060
[33] ATLAS Collaboration, Measurement of the Z/γ^* boson transverse momentum distribution in pp collisions at $\sqrt{s} = 7$ TeV with the ATLAS detector, JHEP 09 (2014) 145. arXiv:1406.3660 [hep-ex], https://doi.org/10.1007/JHEP09(2014)145
[34] H.-L. Lai, et al., New parton distributions for collider physics, Phys. Rev. D 82 (2010) 074024. arXiv:1007.2241 [hep-ph], https://doi.org/10.1103/PhysRevD.82.074024
[35] ATLAS Collaboration, Performance of the reconstruction of large impact parameter tracks in the inner detector of ATLAS, ATL-PHYS-PUB-2017-014, 2017. https://cds.cern.ch/record/2275635.
[36] ATLAS Collaboration, Vertex reconstruction performance of the ATLAS detector at $\sqrt{s} = 13$ TeV, ATL-PHYS-PUB-2015-026, 2015. https://cds.cern.ch/record/2037717.
[37] ATLAS Collaboration, Performance of vertex reconstruction algorithms for detection of new long-lived particle decays within the ATLAS inner detector, ATL-PHYS-PUB-2019-013, 2019. https://cds.cern.ch/record/2669425.
[38] ATLAS Collaboration, Electron and photon performance measurements with the ATLAS detector using the 2015–2017 LHC proton–proton collision data, JINST 14 (2019) P12006. arXiv:1908.00005 [hep-ex], https://doi.org/10.1088/1748-0221/14/12/P12006
[39] ATLAS Collaboration, Electron and photon efficiencies in LHC Run 2 with the ATLAS experiment, JHEP 05 (2024) 162. arXiv:2308.13362 [hep-ex], https://doi.org/10.1007/JHEP05(2024)162
[40] ATLAS Collaboration, Muon reconstruction and identification efficiency in ATLAS using the full Run 2 pp collision data set at $\sqrt{s} = 13$ TeV, Eur. Phys. J. C 81 (2021) 578. arXiv:2012.00578 [hep-ex], https://doi.org/10.1140/epjc/s10052-021-09233-2
[41] ATLAS Collaboration, ATLAS data quality operations and performance for 2015–2018 data-taking, JINST 15 (2020) P04003. arXiv:1911.04632 [physics.ins-det], https://doi.org/10.1088/1748-0221/15/04/P04003
[42] ATLAS Collaboration, Performance of the ATLAS muon triggers in Run 2, JINST 15 (2020) P09015. arXiv:2004.13447 [physics.ins-det], https://doi.org/10.1088/1748-0221/15/09/p09015
[43] ATLAS Collaboration, Performance of electron and photon triggers in ATLAS during LHC Run 2, Eur. Phys. J. C 80 (2020) 47. arXiv:1909.00761 [hep-ex], https://doi.org/10.1140/epjc/s10052-019-7500-2
[44] ATLAS Collaboration, Measurements of Higgs boson production cross-sections in the $H \to \tau^+\tau^-$ decay channel in pp collisions at $\sqrt{s} = 13$ TeV with the ATLAS detector, JHEP 08 (2022) 175. arXiv:2201.08269 [hep-ex], https://doi.org/10.1007/JHEP08(2022)175
[45] ATLAS Collaboration, Search for long-lived, massive particles in events with displaced vertices and missing transverse momentum in $\sqrt{s} = 13$ TeV pp collisions with the ATLAS detector, Phys. Rev. D 97 (2018) 052012. arXiv:1710.04901 [hep-ex], https://doi.org/10.1103/PhysRevD.97.052012
[46] ATLAS Collaboration, Study of the material of the ATLAS inner detector for Run 2 of the LHC, JINST 12 (2017) P12009. arXiv:1707.02826 [hep-ex], https://doi.org/10.1088/1748-0221/12/12/P12009
[47] ATLAS Collaboration, Search for long-lived, massive particles in events with a displaced vertex and a muon with large impact parameter in pp collisions at $\sqrt{s} = 13$ TeV with the ATLAS detector, Phys. Rev. D 102 (2020) 032006. arXiv:2003.11956 [hep-ex], https://doi.org/10.1103/PhysRevD.102.032006
[48] ATLAS Collaboration, Search for long-lived, massive particles in events with displaced vertices and multiple jets in pp collisions at $\sqrt{s} = 13$ TeV with the ATLAS detector, JHEP 06 (2023) 200. arXiv:2301.13866 [hep-ex], https://doi.org/10.1007/JHEP06(2023)200
[49] ATLAS Collaboration, Search for light long-lived particles in pp collisions at $\sqrt{s} = 13$ TeV using displaced vertices in the ATLAS inner detector, Phys. Rev. Lett. 133 (2024) 161803. arXiv:2403.15332 [hep-ex], https://doi.org/10.1103/PhysRevLett.133.161803
[50] ATLAS Collaboration, Search for exotic decays of the Higgs boson into long-lived particles in pp collisions at $\sqrt{s} = 13$ TeV using displaced vertices in the ATLAS inner detector, JHEP 11 (2021) 229. arXiv:2107.06092 [hep-ex], https://doi.org/10.1007/JHEP11(2021)229
[51] C. Borschensky, M. Krämer, A. Kulesza, M. Mangano, S. Padhi, T. Plehn, X. Portell, Squark and gluino production cross sections in pp collisions at $\sqrt{s} = 13, 14, 33$ and 100 TeV, Eur. Phys. J. C 74 (2014) 3174. arXiv:1407.5066 [hep-ph], https://doi.org/10.1140/epjc/s10052-014-3174-y
[52] A.L. Read, Presentation of search results: the CL_s technique, J. Phys. G 28 (2002) 2693. https://doi.org/10.1088/0954-3899/28/10/313
[53] W. Verkerke, D. Kirkby, The RooFit toolkit for data modeling, 2003. arXiv:physics/0306116 [physics.data-an].
[54] W. Beenakker, C. Borschensky, M. Krämer, A. Kulesza, E. Laenen, NNLL-fast: predictions for coloured supersymmetric particle production at the LHC with threshold and Coulomb resummation, JHEP 12 (2016) 133. arXiv:1607.07741 [hep-ph], https://doi.org/10.1007/JHEP12(2016)133
[55] W. Beenakker, C. Borschensky, M. Krämer, A. Kulesza, E. Laenen, V. Theeuwes, S. Thewes, NNLL resummation for squark and gluino production at the LHC, JHEP 12 (2014) 023. arXiv:1404.3134 [hep-ph], https://doi.org/10.1007/JHEP12(2014)023
[56] W. Beenakker, T. Janssen, S. Lepoeter, M. Krämer, A. Kulesza, E. Laenen, I. Niessen, S. Thewes, T. Van Daal, Towards NNLL resummation: hard matching coefficients for squark and gluino hadroproduction, JHEP 10 (2013) 120. arXiv:1304.6354 [hep-ph], https://doi.org/10.1007/JHEP10(2013)120
[57] W. Beenakker, S. Brensing, M. Krämer, A. Kulesza, E. Laenen, I. Niessen, NNLL resummation for squark-antisquark pair production at the LHC, JHEP 01 (2012) 076. arXiv:1110.2446 [hep-ph], https://doi.org/10.1007/JHEP01(2012)076
[58] W. Beenakker, S. Brensing, M. Krämer, A. Kulesza, E. Laenen, I. Niessen, Soft-gluon resummation for squark and gluino hadroproduction, JHEP 12 (2009) 041. arXiv:0909.4418 [hep-ph], https://doi.org/10.1088/1126-6708/2009/12/041
[59] A. Kulesza, L. Motyka, Soft gluon resummation for the production of gluino-gluino and squark-antisquark pairs at the LHC, Phys. Rev. D 80 (2009) 095004. arXiv:0905.4749 [hep-ph], https://doi.org/10.1103/PhysRevD.80.095004
[60] A. Kulesza, L. Motyka, Threshold resummation for squark-antisquark and gluino-pair production at the LHC, Phys. Rev. Lett. 102 (2009) 111802. arXiv:0807.2405 [hep-ph], https://doi.org/10.1103/PhysRevLett.102.111802
[61] W. Beenakker, R. Höpker, M. Spira, P.M. Zerwas, Squark and gluino production at hadron colliders, Nucl. Phys. B 492 (1997) 51. arXiv:hep-ph/9610490, https://doi.org/10.1016/S0550-3213(97)00084-9
[62] J. Butterworth, et al., PDF4LHC recommendations for LHC Run II, J. Phys. G 43 (2016) 023001. arXiv:1510.03865 [hep-ph], https://doi.org/10.1088/0954-3899/43/2/023001
[63] W. Beenakker, et al., Production of charginos, neutralinos, and sleptons at hadron colliders, Phys. Rev. Lett. 83 (1999) 3780. arXiv:hep-ph/9906298, https://doi.org/10.1103/PhysRevLett.83.3780
[64] G. Bozzi, B. Fuks, M. Klasen, Threshold resummation for slepton-pair production at hadron colliders, Nucl. Phys. B 777 (2007) 157. arXiv:hep-ph/0701202, https://doi.org/10.1016/j.nuclphysb.2007.03.052
[65] B. Fuks, M. Klasen, D.R. Lamprea, M. Rothering, Precision predictions for electroweak superpartner production at hadron colliders with resummino, Eur. Phys. J. C 73 (2013) 2480. arXiv:1304.0790 [hep-ph], https://doi.org/10.1140/epjc/s10052-013-2480-0
[66] B. Fuks, M. Klasen, D.R. Lamprea, M. Rothering, Revisiting slepton pair production at the large hadron collider, JHEP 01 (2014) 168. arXiv:1310.2621 [hep-ex], https://doi.org/10.1007/JHEP01(2014)168
[67] J. Fiaschi, M. Klasen, Slepton pair production at the LHC in NLO + NLL with resummation-improved parton densities, JHEP 03 (2018) 094. arXiv:1801.10357 [hep-ex], https://doi.org/10.1007/JHEP03(2018)094
[68] ATLAS Computing Acknowledgements, Technical Report, CERN, Geneva, 2026. https://cds.cern.ch/record/2952666.